Journal of Marine Research, 55, 687–734, 1997

A one-dimensional physical-biological model study of the pelagic nitrogen cycling during the spring bloom in the northern North Sea (FLEX '76)

by Wilfried Kühn[1] and Günther Radach[1]

ABSTRACT

A one-dimensional model of the pelagic ecosystem was developed and applied to the spring bloom in the northern North Sea making use of the data set obtained during the Fladenground experiment FLEX '76. The physical submodel is the second-order turbulence closure model of level 2 type developed by Mellor and Yamada (1974, 1982). The biological submodel is a depth-resolved version of the nitrogen flux model of the lower trophic levels in the pelagic proposed by Fasham *et al.* (1990).

The parameter set employed by Fasham *et al.* did not yield satisfying results. However, using a parameter set adapted to the North Sea ecosystem we obtained a realistic overall description of the development of the North Sea ecosystem during the spring bloom. We were able to hindcast successfully the onset, duration, magnitude and daily variability of the net primary production, the magnitude of the PON export flux to the sea bottom, of the bacterial production and of the nitrogen regeneration within the water column. From the results of the simulation a mass budget of nitrogen fluxes within the euphotic zone and the deeper water layers as well as between them was derived.

The results of the simulation suggest that strong herbivorous grazing caused the decay of the bloom. The comparison with the grazing by mesozooplankton as estimated from the observations favors the hypothesis that herbivorous microzooplankton was mainly responsible for the breakdown.

The depth dependence of the vertical particulate flux obtained from the simulation exhibits the hyperbolic character recently found in different oceanic regions. The vertical particulate nitrogen flux shows a stronger decrease than typically observed for the particulate carbon flux. This is in correspondence with the observation that there was a remarkable increase of the C/N ratio of POM with depth during FLEX '76.

1. Introduction

Marine ecosystem models, which include the interaction of physical and biological processes, are the only tool for investigating on large scales such process-related aspects of important current problems, as understanding and quantification of biogeochemical cycles in the ocean, or the role of the biological pump for regulating the atmospheric carbon dioxide content. This is the reason for the recent trend toward the development of three-dimensional physical-biological models for the application to global or at least basin scales. It is reasonable to support this work by investigations using one-dimensional

1. Institut für Meereskunde, Universität Hamburg, Troplowitzstr. 7, D-22529 Hamburg, Germany.

models which provide the opportunity to study the suitability of different model ecosystem structures, the adequacy of mathematical descriptions of biological or chemical processes and the consequences of special parameter choices with modest computational effort compared to three-dimensional models.

Fasham *et al.* (1990) developed a depth-integrated ecosystem model of the ocean mixed layer. By adjusting certain biological model parameters (especially the mortality rate of phytoplankton) they could reproduce the annual net primary production and its seasonal cycle at Bermuda Station 'S'. When attempting to validate the model by simulating the annual cycle at OWS 'India' in the northeastern Atlantic, Fasham (1993) found it appropriate to replace the linear loss functions of zooplankton and phytoplankton by loss functions varying with biomass. In this way, low zooplankton stocks in winter and early spring with a subsequent unrealistically strong outburst of phytoplankton during the bloom could be avoided. The original version of the biological model was implemented into a general circulation model for the North Atlantic Ocean (Sarmiento *et al.,* 1993; Fasham *et al.,* 1993). The biological results from this 3-D simulation gave a generally adequate description of the geographical patterns, but some serious discrepancies were observed: the concentration of chlorophyll (and of other biological components as well) during the simulated phytoplankton bloom came out too high, the onset of the bloom took place too early, and the deep chlorophyll maximum and the nitracline in summer were markedly shallower than observed. Partly the discrepancies could be traced back to insufficiencies of the hydrodynamical model; e.g., to artificially high horizontal advection or to too shallow summer mixed layers. On the other hand, weaknesses in the biological model were identified. Thus, the too high chlorophyll values during the spring bloom could be at least partly caused by an underestimation of zooplankton biomass in winter and early spring as a consequence of using the linear loss functions mentioned above. This could also explain the overpredicted zooplankton biomass and consequently the overestimated ammonium production in late spring and summer. Additionally, a general overestimation of the nitrate uptake inhibition by ammonium could be partly responsible for the too high nitrate concentrations in depths below 20–30 m at both stations.

Therefore it seemed reasonable to re-examine the biological model used, focusing on the process parameterizations and the parameter values. One possibility for pursuing this investigation is to develop a depth-resolved 1-D ecosystem model based on the same biological structure but with detailed upper layer physics and to apply the model to local situations; e.g., to the development of a spring bloom at a fixed position, for which the necessary data base exists. This was attempted in the present paper by using the data from the Fladenground Experiment performed during spring 1976 in the northern North Sea (FLEX '76).

For simulating the behavior of a pelagic ecosystem, especially the vertical fluxes, a realistic description of the vertical turbulent mixing and stratification processes is an important prerequisite. As long as 3-D models fail to reproduce the horizontal and vertical advection adequately, 1-D models, which concentrate on as stern a description of the

vertical processes as possible, may even be useful for estimating the influence of advective processes. Zero-dimensional models, however, which also neglect the horizontal currents and their influence on the ecosystem, parameterize the vertical physical processes, as turbulent mixing and the development of vertical gradients, in a simple and unreliable way. On the one hand the determination of a realistic time series of mixed layer depths proves to be a highly ambiguous matter, and on the other hand the results of a 0-D model depend critically on the course of the mixed layer depth (Eigenheer *et al.*, 1996). Therefore, it seems much more appropriate to use vertically resolved models as a preliminary stage in the development of reliable 3-D models. As the physical part of our 1-D ecosystem model we used the second-order turbulence-closure model by Mellor and Yamada (1974, 1982) which was recently applied in different coupled physical-biological models (Kühn, 1994; Sharples and Tett, 1994; Oguz *et al.*, 1996).

In Section 2 the most important findings of the Fladenground Experiment are summarized. The physical and the biological submodels used in our simulations are described in Section 3. The results of the physical model concerning the development of the thermal stratification during FLEX '76 are presented and compared with observations in Section 4a. The discussion of the results obtained with the ecosystem model, i.e. the time- and depth-dependent evolution of the biological and chemical state variables is given in Section 4b. The nitrogen fluxes between the compartments and especially the vertical fluxes of particulate nitrogen are presented for different parameter sets in comparison with observations. The last section gives the conclusions and suggestions for further work with the model.

2. The findings from FLEX '76

The Fladenground Experiment 1976 (FLEX '76) in the northern North Sea took place from 26 March to 6 June, 1976 with the purpose of investigating the dynamics of the phytoplankton spring bloom in relation to the physical upper layer dynamics. The position of the central station was 58° 55′ N, 0° 32′ E. The experiment is described in some detail in Lenz *et al.* (1980).

The plankton dynamics observed during FLEX '76 exhibited a 'classical' spring bloom, which started with the onset of the thermal stratification of the water column at 19 April, 1976 (Julian day 110) and declined about 26 days later. The phytoplankton standing stock reached its maximum with 550 mg Chl *a* m^{-2} at about 30 April (Radach *et al.*, 1980). With a C/Chl *a* ratio of 20 this corresponds to a biomass of 11 g C m^{-2}. The main bloom consisted of diatoms, the dominant species group being *Chaetoceros* spp.; phytoflagellates were observed mainly after the diatom bloom constituting a secondary bloom (Wandschneider, 1983).

Parallel to the development of phytoplankton the nitrate concentration in the euphotic zone decreased monotonously by about 8 mmol N m^{-3} from the beginning of the bloom at day 110 until day 127. Neglecting vertical or lateral import one obtains a mean uptake rate of about 0.5 mmol N m^{-3} d^{-1} corresponding to a new production of 40 mg C m^{-3} d^{-1} as

lower estimate. With a mean depth of the euphotic zone of 30 m one obtains an average areal primary production of at least 1.2 g C m^{-2} d^{-1}. Using the ^{14}C method Weigel and Hagmeier (1978) measured a primary production of 1.2 ± 0.5 g C m^{-2} d^{-1} for the same period. Weichart (1980) determined the net primary production during the first 12 days of the bloom (19 April–1 May) from pH value, temperature, salinity and alkalinity and obtained 2.0 g C m^{-2} d^{-1}.

At the beginning of the experiment the ammonium concentration was 0.2 mmol N m^{-3} corresponding to about 2.5% of the nitrate concentration. It started to increase already some days before the bloom, mainly in the upper layer above and near the thermocline, where it reached 2–4 mmol N m^{-3} until the end of the bloom at mid-May (Hammer *et al.*, 1983). This means a large part of the consumed nitrate was converted into ammonium during the two-month period of the bloom.

Before the phytoplankton bloom, the mesozooplankton was dominated by *Euphausiids.* During the bloom copepods began to develop. The biomass of *Calanus finmarchicus* being the most important herbivore during that period increased to 18 g dry weight m^{-2}, i.e. about 130 mmol N m^{-2}, until the beginning of June (Krause and Radach, 1980). Unfortunately, microzooplankton was not measured during FLEX '76. The grazing capacity of the herbivorous mesozooplankton was estimated by Radach *et al.* (1984) to 35–73 g C m^{-2} for the whole investigation period.

The bacterial activity was found to be relatively low during the experiment, the standing stock of bacteria increased from 2 cfu ml^{-1} at 1 May to about 50 cfu ml^{-1} a fortnight later (Hentzschel, 1980). The beginning of the bacterial growth coincided with a sharp decline of the concentration of dissolved free amino acids (DFAA) after a maximum during the exponential growth phase of the phytoplankton (Hammer *et al.*, 1983).

Using moored traps Davies and Payne (1984) measured the sinking flux of particulate organic matter. During the first phytoplankton bloom they determined a POC sedimentation flux at the bottom (150 m) of 185 mg C m^{-2} d^{-1} and a PON flux of 0.6–1.1 mmol N m^{-2} d^{-1}. Integrating over the whole mooring period from 4 April to 3 June, 1976, one obtains from their data a sedimentation flux of about 7.5 g C m^{-2} and about 30–40 mmol N m^{-2}. With a primary production of 36–61 g C m^{-2} (Radach *et al.*, 1984) or 450–770 mmol N m^{-2}, respectively, during that period, the organic carbon flux corresponded to about 12–21% of the primary production. Davies and Payne (1984) themselves gave 20–35% in their paper. The organic nitrogen flux, however, made up only 4–9% of the primary production. Obviously, this difference was due to the increased C/N ratio of 9–18 of the material collected in the near-bottom trap compared to the C/N ratio of 5–8 of particulate matter in the upper layer.

An important question is to which extent the biological dynamics are determined by hydrodynamic effects, like advection and vertical turbulent mixing. A comparison of the surface heat flux and heat storage data indicated a local heat balance, i.e. the net contribution of horizontal advection to the heat budget at the FLEX central station was very low (Friedrich, 1983). That does not, however, exclude an advective influence on the nutrient budget. A closer look into the observations (Eberlein *et al.*, 1980) shows an

increase of the nutrients nitrate, phosphate and silicate after day 128 not only in the upper layer but also in the lower layer. This was ascribed primarily to hydrodynamic (advective) influences by Eberlein *et al.* (1980). Thus, the total period of FLEX '76 can roughly be divided into two phases: a first one spanning about 6 weeks (26 March–7 May) which was only weakly affected by horizontal advection, and a second one (8 May–5 June) where the advective influence was clearly stronger.

The vertical turbulent mixing plays a decisive role. Due to prevailing strong winds and rather low heat input the water column is completely mixed until day 110. The onset of stratification of the upper layer, i.e. the reduction of turbulent mixing, triggered the beginning of the bloom. Later singular storm events with deep mixing (especially at days 133 and 137) provided a replenishment of nutrients in the upper layer thus again fueling new primary production.

3. Model description

The model consists of (1) a vertically resolved physical water column model driven by surface momentum and heat fluxes and absorption of underwater light, and (2) a pelagic ecosystem model driven by solar irradiance and the vertical eddy diffusivities calculated by the physical model. The two parts are described successively.

a. The physical model

First the model equations together with the boundary conditions used are given. The calculation of the forcing functions (surface momentum and heat fluxes) from real meteorological data is described afterward.

i. The model equations. The one-dimensional physical upper layer model developed by Mellor and Yamada (1974) is described by a coupled system of partial differential equations for the horizontal components of momentum and for the temperature:

$$\frac{\partial u}{\partial t} = \frac{\partial}{\partial z}\left[(A_M + \nu_M)\frac{\partial u}{\partial z}\right] + fv,$$

$$\frac{\partial v}{\partial t} = \frac{\partial}{\partial z}\left[(A_M + \nu_M)\frac{\partial v}{\partial z}\right] - fu,$$

$$\frac{\partial T}{\partial t} = \frac{\partial}{\partial z}\left[(A_H + \nu_H)\frac{\partial T}{\partial z}\right] + \frac{1}{\rho c_p}\frac{\partial I}{\partial z}.$$

Here u and v denote the horizontal components of the velocity in eastern and northern directions, respectively, T is the temperature, t the time, z the vertical co-ordinate, f the Coriolis parameter, ρ the density of sea water, c_p the specific heat capacity of sea water at normal conditions, I the intensity of the solar radiation at depth z, A_M and A_H are the depth-dependent vertical eddy diffusivities for momentum and heat and ν_M and ν_H the molecular viscosity and diffusivity, respectively. A further equation for the salinity could easily be added, but we assumed constant salinity because the salinity remained nearly

constant during FLEX '76 (Weichart, 1980; Brockmann *et al.*, 1984). Tidal mixing near the bottom is not taken into account because it does not affect the dynamics of the upper layer.

The boundary conditions at the water surface ($z = 0$) are

$$(A_M + \nu_M)\frac{\partial u}{\partial z}\bigg|_{z=0} = \frac{\tau_x}{\rho},$$

$$(A_M + \nu_M)\frac{\partial v}{\partial z}\bigg|_{z=0} = \frac{\tau_y}{\rho},$$

$$(A_H + \nu_H)\frac{\partial T}{\partial z}\bigg|_{z=0} = \frac{Q_0}{\rho c_p},$$

where τ_x and τ_y denote the components of the wind stress at the water surface in eastern and northern directions, respectively. Q_0 is the net heat flux through the surface, i.e. the sum of latent and sensible heat flux and long-wave back radiation. As boundary conditions for the bottom of the water column ($z = -D$, with $D = 150$ m) constant temperature and vanishing velocities were prescribed:

$$T(-D, t) = T_D,$$
$$u(-D, t) = v(-D, t) = 0.$$

The depth-dependent eddy diffusivities were calculated using stability functions S_M and S_H:

$$A_M = lqS_M$$
$$A_H = lqS_H.$$

Here l denotes a characteristic length scale of turbulent mixing ("mixing length") and $q^2/2$ is the turbulent kinetic energy (TKE). The latter is determined from the diagnostic algebraic equation

$$P + G - \frac{q^3}{B_1 l} = 0,$$

which expresses the main assumption of the level-2 model, namely the local and instantaneous TKE balance of shear production P, buoyancy production G and dissipation $q^3/B_1 l$, (with B_1 an empirical constant). This equation follows from the complete equation for the TKE, if diffusion, advection and time variance of TKE are neglected. The shear and buoyancy production, respectively, of TKE are given by

$$P = lqS_M\left[\left(\frac{\partial u}{\partial z}\right)^2 + \left(\frac{\partial v}{\partial z}\right)^2\right]$$

and

$$G = -lqS_H\,\beta g\frac{\partial T}{\partial z},$$

where β is the (temperature-dependent) thermal expansion coefficient of sea water.

Table 1. Parameters and constants used in the physical water column model.

Symbol	Parameter	Value	Unit	Reference
f	Coriolis parameter	$1.246 \cdot 10^{-4}$	s^{-1}	
g	gravity acceleration	9.81	$m\ s^{-2}$	
ρ	density of sea water	1027	$kg\ m^{-3}$	
c_p	specific heat capacity of sea water	4020	$J\ kg^{-1}\ (°C)^{-1}$	
ν_M	molecular viscosity	$1.34 \cdot 10^{-5}$	$m^2\ s^{-1}$	Mellor and Durbin (1975)
ν_H	molecular diffusivity	$1.34 \cdot 10^{-5}$	$m^2\ s^{-1}$	Mellor and Durbin (1975)
A_1	empirical constant	0.92	dimensionless	Mellor and Yamada (1982)
A_2	empirical constant	0.74	dimensionless	Mellor and Yamada (1982)
B_1	empirical constant	16.60	dimensionless	Mellor and Yamada (1982)
B_2	empirical constant	10.10	dimensionless	Mellor and Yamada (1982)
C_1	empirical constant	0.08	dimensionless	Mellor and Yamada (1982)
β_0	thermal expansion coefficient ($T = 0°C$)	$6.0 \cdot 10^{-5}$	$(°C)^{-1}$	
β_{30}	thermal expansion coefficient ($T = 30°C$)	$3.34 \cdot 10^{-4}$	$(°C)^{-1}$	
α_m	empirical constant for calculating the mixing length	0.2	dimensionless	Mellor (1989)
c_D	drag coefficient	$1.2–1.8 \cdot 10^{-3}$ (dependent on wind velocity)	dimensionless	see Radach and Moll (1993)
c_E	exchange coefficient for latent heat	$1.5 \cdot 10^{-3}$	dimensionless	
c_H	exchange coefficient for sensible heat	$1.3 \cdot 10^{-3}$	dimensionless	
ρ_a	density of air	1.2	$kg\ m^{-3}$	
c_a	specific heat capacity of air	1005	$J\ kg^{-1}\ (°C)^{-1}$	
ζ_1	attenuation coefficient	0.29	m^{-1}	Regener (1992)
ζ_2	attenuation coefficient	0.13	m^{-1}	Regener (1992)
a	weighting factor	0.42	dimensionless	Regener (1992)

The stability functions are depth- and time-dependent functions of the local flux Richardson number R_f and contain five empirical constants A_1, A_2, B_1, B_2, C_1. The values of the latter were taken from Mellor and Yamada (1982) and are listed in Table 1.

The length scale l is approximated in the simplest possible way by the asymptotic

mixing length (Mellor and Durbin, 1975) defined as the ratio of the first and zeroth moment of the turbulence field:

$$l = l_0 = \alpha_m \frac{\int_{-D}^{0} |z| q \, dz}{\int_{-D}^{0} q \, dz}.$$

The empirical constant α_m was set to 0.2 according to Mellor (1989).

The system of differential equations was solved by an implicit difference algorithm. For the time step $n + 1$ the eddy diffusivities were used which had been calculated in the time step n. We found that the stability of the solution depends critically on the criterion

$$\Delta t \leq C^* \frac{(\Delta z)^2}{\max (A_M)},$$

with C^* in the order of one. A vertical resolution in the order of some meters requires time steps of less than 1 min. Generally we used $\Delta z = 2.50$ m and $\Delta t = 20$ sec.

ii. The forcing of the physical model. The model is driven by the surface momentum and heat fluxes which were calculated from standard meteorological observational data (wind velocity, dry and wet air temperature, air pressure) and radiation data. During FLEX '76 the incoming short-wave solar radiation and the long-wave back radiation had been measured (Raschke *et al.,* 1978). Wind stress, sensible and latent heat fluxes were determined from the meteorological data (Brockmann *et al.,* 1984) using the formulae given in the appendix in Radach and Moll (1993). The values for the coefficients are given in Table 1.

For the source term in the temperature equation, the underwater radiation flux, we chose a bimodal exponential absorption function describing the light attenuation in the ocean according to Paulson and Simpson (1977):

$$I(z) = I_0[a \exp (\zeta_1 z) + (1 - a) \exp (\zeta_2 z)].$$

Here I_0 is the flux of global radiation at the sea surface, ζ_1 and ζ_2 are the extinction coefficients for the red and the blue-green spectral ranges, z is the depth ($z < 0$) and a is a weighting factor. During FLEX '76 the percentage depths for the downward radiation flux had been measured by Hoejerslev (1982). Evaluating these data Regener (1992) calculated time- and depth-averaged values of ζ_1, ζ_2 and a for the period of the spring bloom. We used these values as well as a time-varying ζ_2, which describes the influence of phytoplankton

on the light penetration depth. The average values are given in Table 1 together with the other constants and parameter values used in the physical submodel.

b. The ecosystem model

i. Model structure. The ecosystem model uses the biological structure for the lower part of the pelagic food web developed by Fasham *et al.* (1990). It is based on nitrogen because nitrogen supply is regarded as the major limit to biological production in most parts of the oceans. This is assumed to be also valid in the northern North Sea. The model comprises seven compartments: the mineral nutrients nitrate and ammonium, the biotic compartments phytoplankton, zooplankton and bacteria, and the nonliving organic compartments detritus and labile dissolved organic nitrogen (LDON). The effects of higher trophic levels are parameterized by a loss term for the zooplankton.

The compartment phytoplankton comprises all taxonomic groups and size classes. Analogously, the compartment zooplankton represents a mixture of herbivorous, detritivorous and bacterivorous groups thus comprising meso- and microzooplankton. The nonliving particulate organic nitrogen (detritus) consists of phytodetritus, dead zooplankton, fecal pellets and excrements of higher predators. The compartment LDON represents only the low-molecular weight organic nitrogen compounds with turn-over times in the order of hours to days.

Although idealized from a biologist's point of view, the model contains the essential characteristics of the pelagic ecosystem: the 'classical' food chain nutrients—phytoplankton—zooplankton, the pelagic remineralization of particulate nitrogen, both by zooplankton and bacteria, and the microbial loop. In the current version there is no benthic module, i.e. the model does not include the replenishment of nutrients in the water column via benthic remineralization. As long as we intend to simulate only the relatively short period of the phytoplankton spring bloom, this is not a serious restriction.

The differences between our model and Fasham's improved integral model version (model B in Fasham, 1993) can be characterized as follows:

- The model is vertically resolved; it is a differential one.
- The physical forcing of the biological submodel is supplied—apart from the solar radiation—by depth- and time-dependent vertical eddy diffusivities instead by the temporally variable mixed-layer depth.
- Besides sinking of detritus and transport by vertical turbulent diffusion, sinking of phytoplankton is taken into account as an additional export process.
- Particulate organic matter supplied by higher predators is not immediately exported out of the mixed layer but is added to the detritus pool which is sinking with a prescribed velocity.
- The limitation function for nutrient uptake by phytoplankton used by Fasham (1993)

parameterizing the ammonium-induced inhibition of nitrate uptake according to Wroblewski (1977), has been replaced by the limitation function for the simultaneous uptake of two substitutable nutrients according to O'Neill *et al.* (1989).

ii. Model equations. The temporal and spatial changes of the seven state variables are described by the following system of partial differential equations:

$$\frac{\partial P}{\partial t} = (1-\gamma)\sigma(I_0^*, P, N_n, N_r)P - G_1 - \mu_1 \frac{P}{K_5+P}P - w_p \frac{\partial P}{\partial z} - \frac{\partial}{\partial z}\left((A_M + \nu_M)\frac{\partial P}{\partial z}\right)$$

$$\frac{\partial Z}{\partial t} = \beta(G_1 + G_2 + G_3) - \mu_2 \frac{Z}{K_6+Z}Z - \frac{\partial}{\partial z}\left((A_M + \nu_M)\frac{\partial Z}{\partial z}\right)$$

$$\frac{\partial B}{\partial t} = U_1 + U_2 - G_2 - \mu_3 B - \frac{\partial}{\partial z}\left((A_M + \nu_M)\frac{\partial B}{\partial z}\right)$$

$$\frac{\partial D}{\partial t} = (1-\beta)(G_1 + G_2) - \beta G_3 - \mu_4 D + \mu_1 \frac{P}{K_5+P}P + (1-\epsilon-\delta)\mu_2 \frac{Z}{K_6+Z}Z - w_d \frac{\partial D}{\partial z} - \frac{\partial}{\partial z}\left((A_M + \nu_M)\frac{\partial D}{\partial z}\right)$$

$$\frac{\partial N_n}{\partial t} = -F(I_0^*, P)Q_1(N_n, N_r)P - \frac{\partial}{\partial z}\left((A_M + \nu_M)\frac{\partial N_n}{\partial z}\right)$$

$$\frac{\partial N_r}{\partial t} = -F(I_0^*, P)Q_2(N_n, N_r)P - U_2 + \mu_3 B + \epsilon\mu_2 \frac{Z}{K_6+Z}Z - \frac{\partial}{\partial z}\left((A_M + \nu_M)\frac{\partial N_r}{\partial z}\right)$$

$$\frac{\partial N_d}{\partial t} = \gamma\sigma(I_0^*, P, N_n, N_r)P + \mu_4 D + \delta\mu_2 \frac{Z}{K_6+Z}Z - U_1 - \frac{\partial}{\partial z}\left((A_M + \nu_M)\frac{\partial N_d}{\partial z}\right).$$

Here P denotes the phytoplankton, Z the zooplankton, B the bacteria, D the detritus, N_n the nitrate, N_r the ammonium and N_d the labile dissolved organic nitrogen (LDON). All state variables are concentrations, the unit of which is mmol N m^{-3}. The last terms in all equations represent the turbulent and molecular diffusion.

The biological terms will be briefly explained in the following. A more detailed discussion of these terms can be found in Fasham *et al.* (1990) and in Fasham (1993), respectively.

Phytoplankton equation. The first term describes the photosynthesis of the phytoplankton as product of the growth rate and the standing crop, diminished by a constant fraction γ representing the exudation of LDON. The gross growth rate σ is expressed as product of a light-dependent growth rate and a (dimensionless) nutrient limitation function:

$$\sigma(I_0^*, P, N_n, N_r) = F(I_0^*, P)Q(N_n, N_r).$$

The depth- and time-dependent light-limited growth rate F is described by the expression

$$F(z, t) = \frac{V_p \, \alpha \, I^*(z, t)}{(V_p^2 + \alpha^2 I^{*2}(z, t))^{1/2}},$$

where V_p is the maximum specific growth rate of phytoplankton, α the initial slope of the light-production curve and I^* the photosynthetically available radiation (PAR) intensity at a given depth. The latter depends on the intensity at the water surface $I_0^* = I^*(z = 0)$, on the extinction by the water including yellow substances and suspended inorganic matter (k_w) and on the self-shading by the phytoplankton (k_c):

$$I^*(z, t) = I_0^*(t) \exp [(k_w z + k_c \int_0^z P(z', t) \, dz'].$$

This expression corresponds to the second term in the absorption function used in the physical model when a time-dependent attenuation coefficient ζ_2 is used, i.e.

$$\zeta_2(t) = k_w + k_c \frac{1}{z} \int_0^z P(z', t) dz'.$$

The growth limitation by the nutrient concentrations is described by the function:

$$Q(N_n, N_r) = Q_1(N_n, N_r) + Q_2(N_n, N_r)$$

with

$$Q_1(N_n, N_r) = \frac{N_n/K_1}{1 + N_n/K_1 + N_r/K_2}$$

and

$$Q_2(N_n, N_r) = \frac{N_r/K_2}{1 + N_n/K_1 + N_r/K_2}.$$

This limitation function was developed by O'Neill *et al.* (1989) to describe the simultaneous uptake of two substitutable nutrients (here nitrate and ammonium): Different affinities of the phytoplankton for the two nutrients are expressed by different half-saturation constants K_1 and K_2. The inhibition of the uptake of one nutrient by the presence of the other is contained implicitly.

The model uses the balanced-growth assumption, i.e. nutrient uptake rate and growth rate are viewed as identical. Internal nutrient pools which allow uptake without immediate growth as well as increase of biomass without nutrient uptake are not taken into account.

The second and the third term in the phytoplankton equation describe the losses by

zooplankton grazing and by natural mortality, respectively. The fourth term describes the sinking of the phytoplankton.

Zooplankton equation. The first term in the equation describes the grazing of the model zooplankton on the different available food sources: phytoplankton, bacteria and detritus. The partial grazing rates Gi (i = 1,3) are calculated as Michaelis-Menten functions of the available food $F = F^N = \sum_i p_i X_i$, where the weighting factors p_i (with $\sum_i p_i = 1$) are the grazing preferences of the zooplankton for the various food types X_i ($X_1 = P$, $X_2 = B$, $X_3 = D$):

$$G_i = G_i^T = g \frac{p_i X_i}{K_3 + \sum_j p_j X_j} Z.$$

Here g is the maximum specific grazing or ingestion rate and K_3 the half-saturation constant for ingestion (Tilman, 1982). If the preferences p_i themselves are assumed to be proportional to the relative food shares (Hutson, 1984),

$$p_i = \frac{\rho_i X_i}{\sum_j \rho_j X_j} \left(\text{with} \sum_j \rho_j = 1 \right),$$

one obtains for the partial grazing rates:

$$G_i = G_i^H = g \frac{\rho_i X_i^2}{K_3 \sum_j \rho_j X_j + \sum_j \rho_j X_j^2} Z.$$

The factors ρ_i are the grazing preferences for the different food sources X_i which apply when the concentrations of these food sources are equal. This grazing function ensures that the model zooplankton dynamically adapts its grazing to the available food by overproportional feeding of the most abundant food type ("frequency dependent switching of feeding"). The latter expression, which had been used by Fasham *et al.* (1990), is also applied in our simulations. We also tested, however, in a special process study the consequences of substituting the grazing rates G_i^H by G_i^T. We found that with the Hutson function the realized grazing rates are less dependent on the prescribed preferences than with the Tilman function. This motivated the choice of the former in our simulations. The partial grazing rates are multiplied with the assimilation efficiency β; the fraction 1-β of ingested food is the egestion of fecal pellets.

The second term in the zooplankton equation describes the total losses due to excretion of dissolved metabolic products (LDON and ammonium) and due to natural mortality and predation by higher predators. As proposed by Fasham (1993) the loss rates of phytoplankton and zooplankton are Michaelis-Menten functions of the biomass. In the loss terms μ_1

and μ_2 denote the maximum specific loss rates; K_5 and K_6 are the half-saturation constants for phytoplankton and zooplankton losses, respectively.

Vertical migration of the zooplankton and the parallel diurnal rhythm of grazing were not taken into account, because the observations during FLEX '76 had shown that *C. finmarchicus* started to migrate not before mid-May (Krause and Radach, 1989).

Bacteria equation. The mathematical description of the bacterial growth takes into account that marine bacteria do not only consume low-molecular weight compounds (LDON) and excrete ammonium, but that they are able to take up ammonium as additional nitrogen source, i.e. that they can behave simultaneously as nitrogen regenerators and competitors for the phytoplankton with respect to ammonium (Tupas and Koike, 1991). The uptake of LDON (U_1) and of ammonium (U_2) by heterotrophic microbes is parameterized according to Fasham *et al.* (1990). The third term in the bacteria equation describes the loss due to grazing by zooplankton. The excretion of ammonium is given by the fourth term and is assumed to be proportional to the bacterial biomass (excretion rate μ_3).

Detritus equation. Sources of detritus are the production of fecal pellets assumed as a fixed part of the zooplankton ingestion (first term), the phytoplankton mortality (fourth term) and a certain part of the zooplankton losses (fifth term). Sinks are zooplankton grazing on detritus (second term) and the biochemical decay to LDON, the latter being described as a first-order reaction with a constant breakdown rate μ_4 (third term). The sixth term in the equation describes the sinking of detritus with a constant velocity w_d.

Nitrate equation. The equation describes nitrate uptake by phytoplankton and the diffusion of nitrate. Neither pelagic nor benthic nitrification is taken into account. The primary production utilizing nitrate is considered as new production.

Ammonium equation. The first two terms represent the ammonium uptake by phytoplankton and by bacteria, respectively. Sources of ammonium are the bacterial excretion (third term) and a certain fraction (ϵ) of zooplankton losses due to excretion and mortality (fourth term). The primary production utilizing ammonium is considered as regenerated production.

LDON equation. The sources for labile DON are the exudation by the phytoplankton (first term), the decay of detritus (second term) and a certain fraction (δ) of zooplankton losses (third term). The only biological sink for LDON is the bacterial uptake (fourth term).

Boundary conditions. No-flux conditions are prescribed for all state variables at the air-sea interface ($z = 0$):

$$\left.\frac{\partial X_i}{\partial z}\right|_{z=0} = 0 \qquad \text{for } X_i = Z, B, N_n, N_r, N_d$$

and

$$A_M \frac{\partial P}{\partial z}\bigg|_{z=0} = w_p P, \qquad A_M \frac{\partial D}{\partial z}\bigg|_{z=0} = w_d D.$$

For the bottom ($z = -D$) the boundary conditions are

$$\frac{\partial X_i}{\partial z}\bigg|_{z=-D} = 0 \qquad \text{for } X_i = P, Z, D, B, N_n, N_r, N_d.$$

The differential equations were solved using an explicit algorithm. By restricting the vertical turbulent diffusivities to $\leq 0.2\ m^2\ s^{-1}$ we could use the same time step as for the physical model. The influence of this prescription is, however, negligible, because diffusivities $>0.2\ m^2\ s^{-1}$ occur only during the first few days of the simulation period.

iii. Parameter values and initial conditions: Parameter values. The two different parameter sets we used are given in Table 2. Parameter set NA is nearly identical with the parameter set of model B in Fasham (1993). One exception is the maximum growth rate of phytoplankton V_p which was chosen as $1.5\ d^{-1}$ according to the mean temperature in the mixed layer. This value is also the upper limit of the growth rates given by Schöne (1977) for the diatom *Chaetoceros debilis* ($V_p = 1.2 - 1.5\ d^{-1}$). Furthermore, the sinking velocity for detritus was chosen as $w_d = 3\ m\ d^{-1}$ in order to reproduce the measured PON sedimentation flux.

The second parameter set NS exhibits a series of modifications which take into account observations in the North Sea or includes changes of parameter values which proved to be necessary in the course of data fitting. Before the onset of the bloom the extinction coefficient of the water in the FLEX region was $k_w = 0.09\ m^{-1}$ (Hoejerslev, 1982). The slope α of the P-I curve was determined during the Fladenground experiment by Mommaerts (see Brockmann *et al.*, 1984). From his data a mean value of $\alpha = 0.013$ mg C (mg Chl *a*)$^{-1}$ h^{-1} (μE m^{-2} s^{-1})$^{-1}$ follows for the main phase of the bloom. Using the Chl *a*/C ratio of 20 and the conversion factor between the amount of PAR (measured in μE) and transported energy (measured in Ws) of 1 Ws = 4.15 μE for underwater light (Morel and Smith, 1974) one obtains $\alpha = 0.065\ d^{-1}\ (W\ m^{-2})^{-1}$. The half-saturation constants for nitrate and ammonium uptake were chosen as $K_1 = 0.2$ mmol N m^{-3} and $K_2 = 0.8$ mmol N m^{-3}, respectively. This choice follows from a special investigation of the consequences of using different affinities on which we will report elsewhere. For the assimilation efficiency of the zooplankton we used $\beta = 0.625$ as given by Butler *et al.* (1970) for the copepod *Calanus finmarchicus,* the dominant mesozooplankton species in the northern North Sea.

The maximum bacterial uptake rate was reduced to $V_b = 1.2\ d^{-1}$ according to the prevailing lower temperature. This corresponds to the finding of Hentzschel (1980) that the microbial activity during FLEX '76 was rather low. The excretion rate of the bacteria was increased to $0.15\ d^{-1}$ to obtain a growth efficiency in the order of 50% (Billen *et al.*, 1990). The exclusion of ammonium uptake by the bacteria ($\eta = 0$) expresses our assumption that

Table 2. Parameters of the biological model. NA denotes the North Atlantic parameter set according to Fasham (1993)—model B with the two exceptions printed in italics (see text); NS denotes the North Sea parameter set. Bold numbers mark the values in set NS differing from those in set NA.

Symbol	Parameter	Value set NA	Value set NS	Unit
phytoplankton:				
k_w	extinction coefficient of water	0.04	**0.09**	m^{-1}
k_c	selfshading coefficient	0.03	0.03	m^2 (mmol N)$^{-1}$
V_p	maximum specific uptake rate	*1.50*	1.50	d^{-1}
α	slope of the P-I-curve (I $\rightarrow$ 0)	0.025	**0.065**	m^2 (W d)$^{-1}$
K_1	half saturation constant nitrate uptake	0.5	**0.2**	mmol N m^{-3}
K_2	half saturation constant ammonium uptake	0.5	**0.8**	mmol N m^{-3}
μ_1	mortality rate	0.05	0.05	d^{-1}
K_5	half-saturation constant mortality	0.2	0.2	mmol N m^{-3}
γ	exudation fraction	0.05	0.05	dimensionless
Ψ	inhibition parameter	1.5	—	m^3 (mmol N)$^{-1}$
w_p	sinking velocity	—	**1.0**	m d^{-1}
zooplankton:				
g	maximum ingestion rate	1.0	1.0	d^{-1}
K_3	half saturation constant ingestion	1.0	1.0	mmol N m^{-3}
β	assimilation efficiency	0.75	**0.625**	dimensionless
μ_2	maximum loss rate	0.3	0.3	d^{-1}
K_6	half saturation constant losses	0.2	0.2	mmol N m^{-3}
δ	LDON fraction of losses	0.2	**0.1**	dimensionless
ϵ	NH_4 fraction of losses	0.7	0.7	dimensionless
ρ_1	grazing preference for phytoplankton	0.5	**0.55**	dimensionless
ρ_2	grazing preference for bacteria	0.25	**0.40**	dimensionless
ρ_3	grazing preference for detritus	0.25	**0.05**	dimensionless
bacteria:				
V_b	maximum uptake rate	2.0	**1.2**	d^{-1}
K_4	half saturation constant uptake	0.5	0.5	mmol N m^{-3}
μ_3	excretion rate	0.05	**0.15**	d^{-1}
η	uptake ratio NH_4:LDON	0.6	**0.0**	dimensionless
detritus:				
μ_4	breakdown rate	0.05	**0.02**	d^{-1}
w_d	sinking velocity	*3.0*	**2.0**	m d^{-1}

dissolved free amino acids with a low C/N ratio of $\leq$4 (Hammer *et al.*, 1983) were the main nitrogen source for the bacteria.

In order to approximately reproduce the sinking flux of PON measured in a depth of 150 m we had to choose a mean sinking velocity of 2 m d^{-1} for detritus and 1 m d^{-1} for

Table 3. Initial values of the biological state variables (in mmol N m^{-3}) for day 97.0, i.e. 7 April, 1976, 0 h.

State variable	Initial concentration
phytoplankton (PHY)	0.10 (0–20 m)
	0.05 (20–150 m)
zooplankton (ZOO)	0.05 (0–150 m)
bacteria (BAC)	0.001 (0–150 m)
detritus (DET)	0.50 (0–100 m)
	linearly decreasing to 0.0 (100–150 m)
nitrate (NIT)	8.30
ammonium (AMM)	0.22
labile dissolved organic nitrogen (LDON)	0.14

(living) phytoplankton. To maintain the rather high concentration of PON (especially fecal pellets) which was observed during FLEX '76 we lowered the decay rate of detritus ($\mu_4 = 0.02\ d^{-1}$) and the grazing preference of zooplankton for detritus (ρ_3). For the same reason the detrital fraction of the zooplankton losses ($1 - \epsilon - \delta$) was increased from 0.1 to 0.2 by lowering the LDON fraction δ.

To sum up, the parameters printed in bold letters in Table 2 were modified in comparison with the values in parameter set NA. The implications of these changes are:

- The intensity of the underwater light is reduced due to higher basic extinction but the phytoplankton is better adapted to low light levels.
- The nitrate uptake by phytoplankton is favored to the disadvantage of the ammonium uptake.
- The growth efficiency of zooplankton is somewhat reduced, its 'virtual' preferences for phytoplankton and bacteria are distinctly higher than for detritus (but one has to keep in mind that the real preferences strongly depend on the food supply).
- The bacteria grow more slowly and with lower efficiency; they act only as regenerators and not as consumers of mineral nitrogen.
- The detritus decays more slowly.

Initial conditions. The initial concentrations (in mmol N m^{-3}) for day 97.0 are given in Table 3. The initial depth profiles of phytoplankton, nitrate and ammonium were deduced from the depth-time contour plots of the observations during FLEX '76. As an initial condition for the zooplankton the depth-averaged biomass concentration for *C. finmarchicus* was chosen because the total biomass of zooplankton had not been determined during FLEX '76. The initial detritus concentration was obtained from depth profiles of PON. As an initial value of LDON, the observed concentration of dissolved free amino acids (DFAA) was used; other labile organic nitrogen compounds were not taken into account

due to the lack of data. The bacterial biomass concentration was estimated from bacterial counts (in cfu ml^{-1}) made during FLEX '76.

4. Results and discussion

a. Simulation of the development of stratification and thermocline

The basic forcing variables for the physical water column model were the wind velocity and the solar radiation (Fig. 1a,b).

The simulated development of the vertical thermal stratification in the water column during FLEX '76 is shown in Figure 2a. The observed temperature profiles obtained from CTD data (Brockmann *et al.,* 1984) are given in Figure 2b. The agreement is very satisfactory. Especially the onset of stratification around day 110 due to weakening wind and increasing solar irradiance is well reproduced by the simulation. In the second half of the simulation period, however, the width of the thermocline is underestimated by the simulation (by about 10 m at day 160). The rms deviation between simulated and observed temperatures calculated over the whole simulation period and over a depth of 50 m amounts to only 0.23°C. We want to stress that this result was obtained without any tuning of model parameters. We used the originally measured wind velocities without any corrections. The good agreement between simulation and observation becomes especially evident when we compare the development of the near-surface temperature (Fig. 1c). The rms deviation between the two curves amounts to 0.16°C at a temperature rise of 3.5°C during the two months. It is noteworthy that these results were obtained using constant light attenuation coefficients. A test run with temporally varying coefficients (characteristic for a plankton bloom) yielded only negligible differences.

Information on the vertical mixing regime is presented in Figure 3. The temporal development of the vertical eddy diffusion coefficient in the surface layer is given in Figure 3a. Very high values of $A_M(z = 7.25\ \text{m})$ are characteristic for the period before day 110 due to the strong storms and the low global radiation. The depth-time profile of the vertical eddy diffusion coefficient is shown in Figure 3b. The isoline $A_M = 1.5\ 10^{-5}\ m^2\ s^{-1}$ denotes the transition from turbulent to molecular (background) mixing. The temporal evolution of the mixed-layer depth during that time is shown in Figure 1d. Obviously, the transition from the fully mixed water column to a stratified one at day 110 as well as the overall development of the mixed layer afterward are quite well reproduced by the model. Differences between the mixed-layer depths determined from the observed and the simulated temperature profiles, respectively, do exist on the scale of a few days. The mixed-layer depth is defined here as the depth at which the temperature is 0.2°C lower than the surface temperature (Mellor, 1989). If we apply a temperature gradient criterion for determining the mixed-layer depth, we obtain a somewhat different picture of the mixed-layer depth evolution. This reflects the well-known difficulty to define and to determine the mixed-layer depth unambiguously. Amongst other reasons this is a strong argument against the use of integral, zero-dimensional ecosystem models with the mixed-layer depth as a physical forcing variable. Eigenheer *et al.* (1996) could exemplify

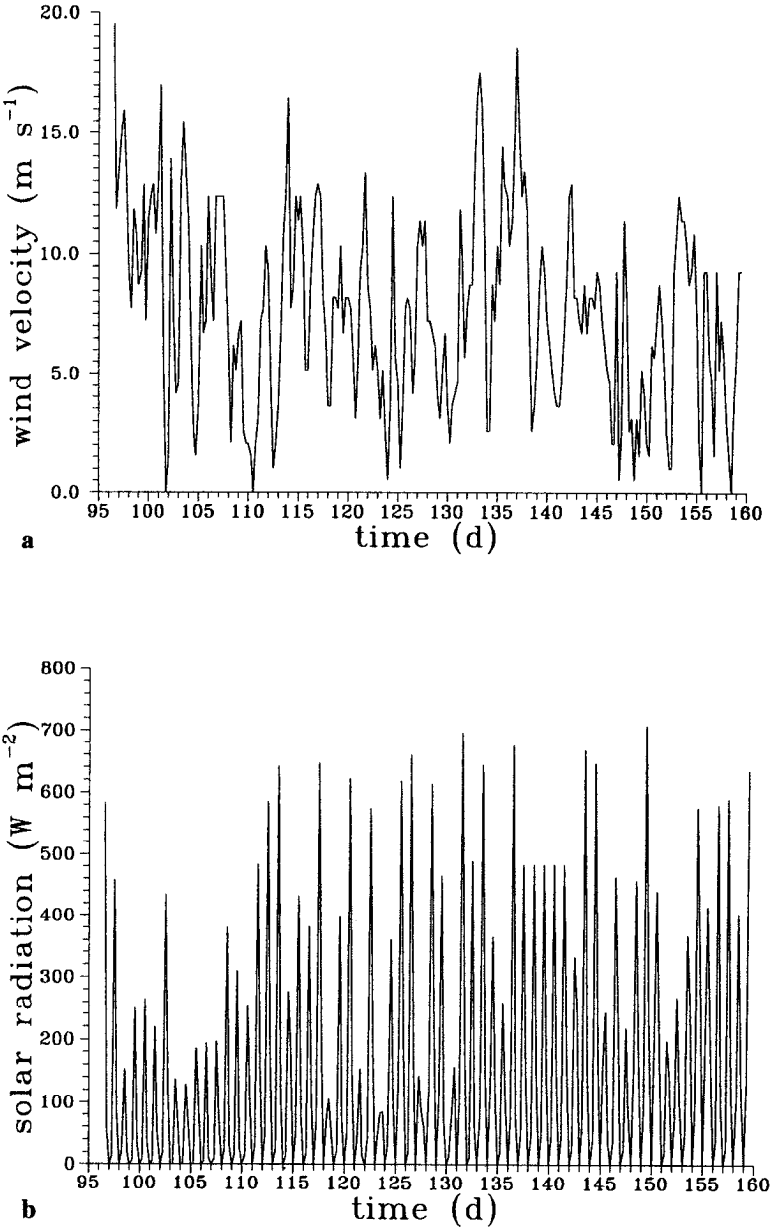

Figure 1. The major meteorological forcing data: (a) wind velocities and (b) solar radiation as measured during FLEX '76 (Brockmann *et al.*, 1984); (c) development of the SST during FLEX '76—comparison of simulation and observation (Brockmann *et al.*, 1984); (d) mixed-layer depth during FLEX '76, as determined from CTD data and from the simulated temperature profiles, respectively, using a difference criterion.

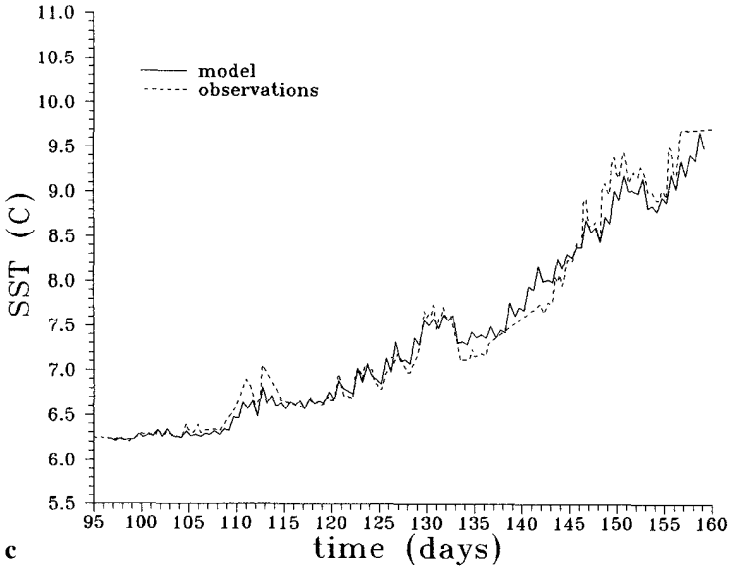

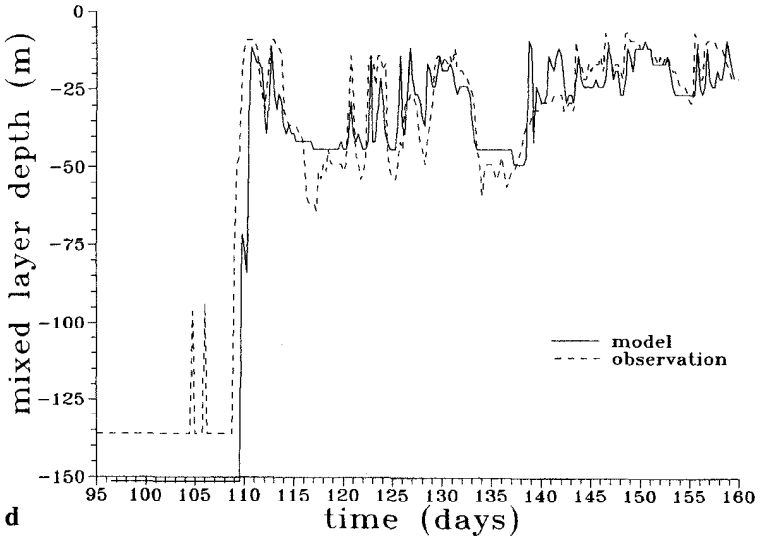

Figure 1. (Continued)

this by investigating the influence of different time series of mixed-layer depths obtained by different definitions on the biological results when using the integral Fasham model to describe the development of the spring bloom observed during FLEX '76 in the northern North Sea.

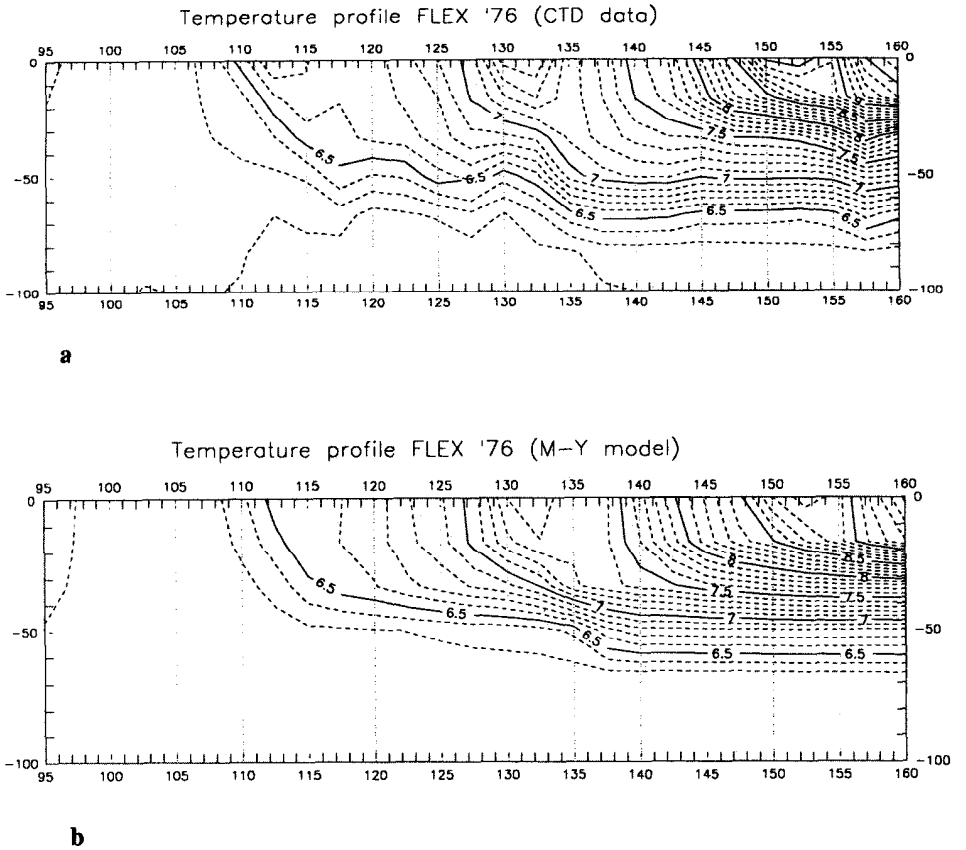

Figure 2. Development of the thermal stratification in the upper 100 m of the water column during FLEX '76: (a) observation (Brockmann *et al.*, 1984), (b) simulation.

The net heat input into the water column calculated from the simulated heat and radiation fluxes through the surface, amounts to $4.9 \cdot 10^8$ J m^{-2}. Friedrich (1983) determined an increase of the heat content in the water column of $5.0 \cdot 10^8$ J m^{-2} from the measured temperature profiles. This means that the net contribution of horizontal advection to the heat budget at the FLEX central station was negligibly small. Obviously, the thermal structure of the water column was mainly determined by vertical processes which are well described by the physical model. Thus we have an ideal case for the application of a one-dimensional ecosystem model.

b. Simulation of the ecosystem dynamics during the spring bloom

i. Comparison of simulations with parameter sets NA and NS. The simulations made by Sarmiento *et al.* (1993) with the 3-D coupled circulation-ecosystem model of the North Atlantic using the parameter set given by Fasham (1993) did not include the shelf seas.

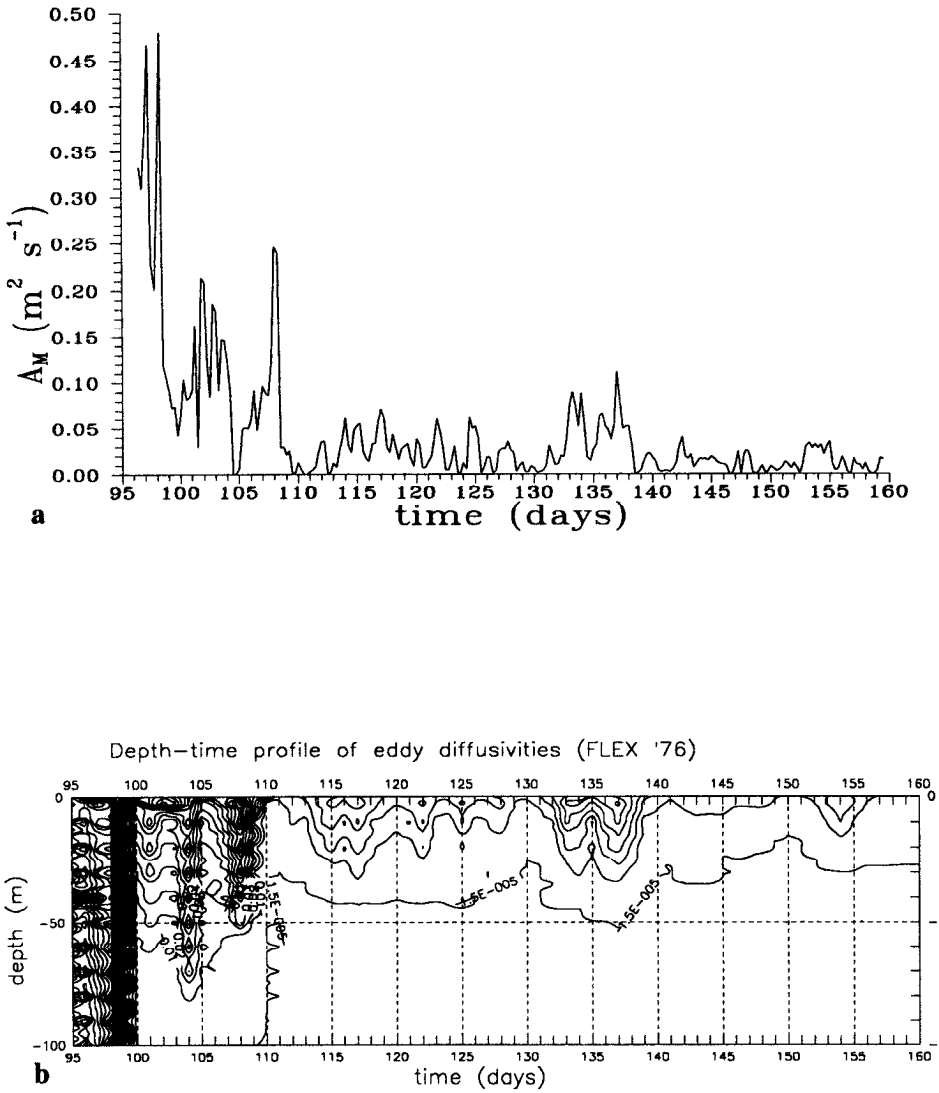

Figure 3. Vertical eddy diffusion coefficient in the surface layer; (b) depth-time profile of the eddy diffusion coefficients in the upper 100 m.

This is due to the rather coarse horizontal resolution of the model. But it seems to be essential to include the biologically high productive marginal seas when a realistic assessment of global fluxes of carbon, nitrogen and other essential elements is intended. Therefore we investigated the differences between simulations using the 'universal' parameter set NA used to describe the biological processes in the open North Atlantic (Fasham, 1993) with the two exceptions mentioned and the parameter set NS adapted to shelf sea conditions.

Table 4. Depth- and time-integrated nitrogen fluxes as obtained from simulations NA and NS for FLEX '76. Integration depth: 150 m, simulation period: 7 April–7 May (days 97.0–128.0) and 7 April–4 June, 1976 (days 97.0–156.0). Unit: mmol N m^{-2} (time span)$^{-1}$. PHY: phytoplankton, ZOO: zooplankton, BAC: bacteria, DET: detritus, AMM: ammonium, NIT: nitrate, LDON: labile dissolved organic nitrogen.

		Short time range (days 97.0–128.0)		Long time range (days 97.0–156.0)	
Process	Acronym	Run NA	Run NS	Run NA	Run NS
NIT uptake by PHY	NUPTAP	236	318	266	380
AMM uptake by PHY	AUPTAP	71	39	260	207
LDON exudation by PHY	PEXUDL	15	18	26	29
mortality PHY	PMORTD	47	62	67	85
sinking PHY	PSINKP	0	1	0	2
ZOO grazing on PHY	PGRAZZ	222	231	400	432
ZOO grazing on BAC	BGRAZZ	94	9	286	59
ZOO grazing on DET	DGRAZZ	88	40	236	311
total losses ZOO	ZLOSST	204	109	639	463
production of fecal pellets	ZFECPD	101	105	231	301
decay of DET to LDON	DSOLUL	66	40	120	99
loss ZOO as DET	ZLOSSD	20	22	64	93
sinking DET	DSINKD	18	17	24	26
loss ZOO as LDON	ZLOSSL	41	11	128	46
LDON uptake by BAC	LUPTAB	139	78	292	180
AMM uptake by BAC	AUPTAB	83	0	175	0
loss ZOO as AMM	ZLOSSA	143	76	448	324
AMM excretion by BAC	BEXCRA	67	40	130	106

The results of both simulations are presented in Table 4. All nitrogen fluxes are depth-integrated over the whole water depth and time-integrated from day 97.0 until day 128.0 and day 156.0, respectively. The turbulent diffusion terms have been omitted because their integral over the total water depth is zero. From both model outputs we extracted important characteristics, which are suitable for comparison with observations (Table 5).

As stated above, the simulated net primary production given as the sum of nitrate and ammonium uptake by phytoplankton has a realistic order of magnitude. But as can be seen from Figure 4a, in run NA the depletion of the nitrate pool in the euphotic zone (0–30 m) is too weak. We have to conclude that ammonium uptake is overestimated by model run NA. This is mainly caused by the special parameterization of nitrogen uptake by phytoplankton according to Wroblewski (1977) with a too strong inhibition of nitrate uptake by ammonium. Also the bacterial production and the growth efficiency of the bacteria came out too high (Table 5). The rather small ratio between the amounts of LDON exuded by phytoplankton and taken up by bacteria also suggests an overestimation of bacterial activity in simulation NA. This is confirmed by the too early and too strong development of bacterial biomass and the total exhaustion of the LDON pool after a few days (not shown).

Table 5. Characteristic quantities obtained from simulations NA and NS in comparison with observational values taken from the literature. (1) measurements by Weigel and Hagmeier (1978) (Radach *et al.*, 1984); Mommaerts (1981); (2) Hammer *et al.* (1983); (3) Cole *et al.* (1988); (4) Billen *et al.* (1990); (5) Radach *et al.* (1984); (6) Davies and Payne (1984).

	Short time period (days 97.0–128.0)			Long time period (days 97.0–156.0)			
	Run NA	Run NS	Observation	Run NA	Run NS	Observation	Ref.
NPP (mmol N m^{-2})	307	358	250–365	526	587	450–770	(1)
NPP (g C m^2)	24.4	28.5	20–29	41.8	46.7	36–61	(1)
new production (mmol N m^{-2})	236	318	≥315	266	380		(2)
f-ratio	0.77	0.89	0.86–1.00	0.51	0.65		
bacterial net production BNP (mmol N m^{-2})	155	38	50–110	336	74	90–230	(3)
BNP/NPP	50%	11%	20–30%	64%	13%	20–30%	(3)
bacterial growth efficiency	70%	49%	≤50%	72%	41%	≤50%	(4)
exudation PHY/bacterial LDON uptake	11%	23%	≤20%	9%	16%	≤20%	(4)
total grazing (mmol N m^{-2})	404	280	65–125	922	802	440–920	(5)
total grazing (g C m^{-2})	32.1	22.3	5–10	73.3	63.8	35–73	(5)
PHY grazing/total grazing	55%	83%		43%	54%		
BAC grazing/total grazing	23%	3%		31%	7%		
DET grazing/total grazing	22%	14%		26%	39%		
PON export (mmol N m^{-2})	18	19	12–13	24	28	30–40	(6)
PON export/NPP	6%	5%	3–4%	4%	5%	4–9%	(6)
PON export/new production	7%	6%	4–5%	9%	7%		
PON storage/new production	76%	73%		44%	35%		
AMM storage/new production	24%	24%		54%	59%		

Thus, simulation NA reveals that the order of magnitude of net primary production in the northern North Sea during spring can be estimated quite well using the North Atlantic parameter set. New production, however, is underestimated in favor of regenerated production.

Now we discuss the results of the simulation with the parameter set NS using the depth-time distributions of the state variables (Fig. 5a–g) and the depth- and time-integrated processes (Fig. 6a–g). In the latter figures the nitrogen fluxes are integrated over

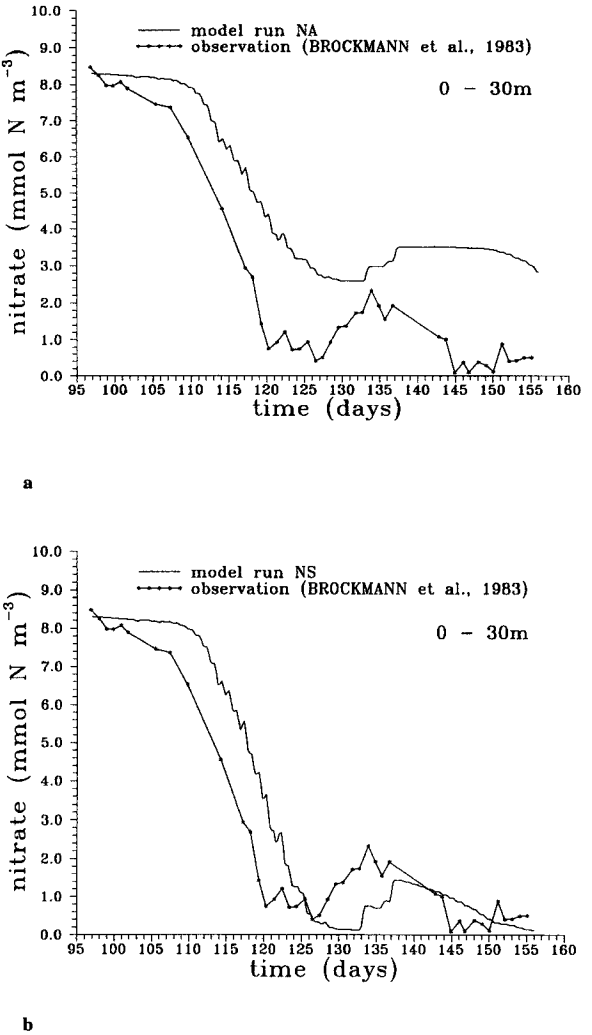

Figure 4. Nitrate concentration in the upper 30 m as obtained from model run NA in comparison with observation (Brockmann *et al.*, 1983); (b) the same for model run NS.

the euphotic zone, with positive and negative shares displayed separately. The simulation period begins at day 97.0, i.e. 7 April, 1976, 0 h. About 13 days later, at day 110, the bloom starts to develop. At the beginning of May the phytoplankton standing stock reaches its first maximum, afterward decreasing rapidly due to increasing grazing pressure by the zooplankton (Fig. 5a, 6a). After day 140 a second, weaker bloom develops mainly due to increasing ammonium uptake. About one week after the first phytoplankton peak the bacterial stock reaches its highest value (Fig. 5c), only a few days later followed by the zooplankton (Fig. 5b). Zooplankton and bacteria exhibit the highest concentrations always in the upper

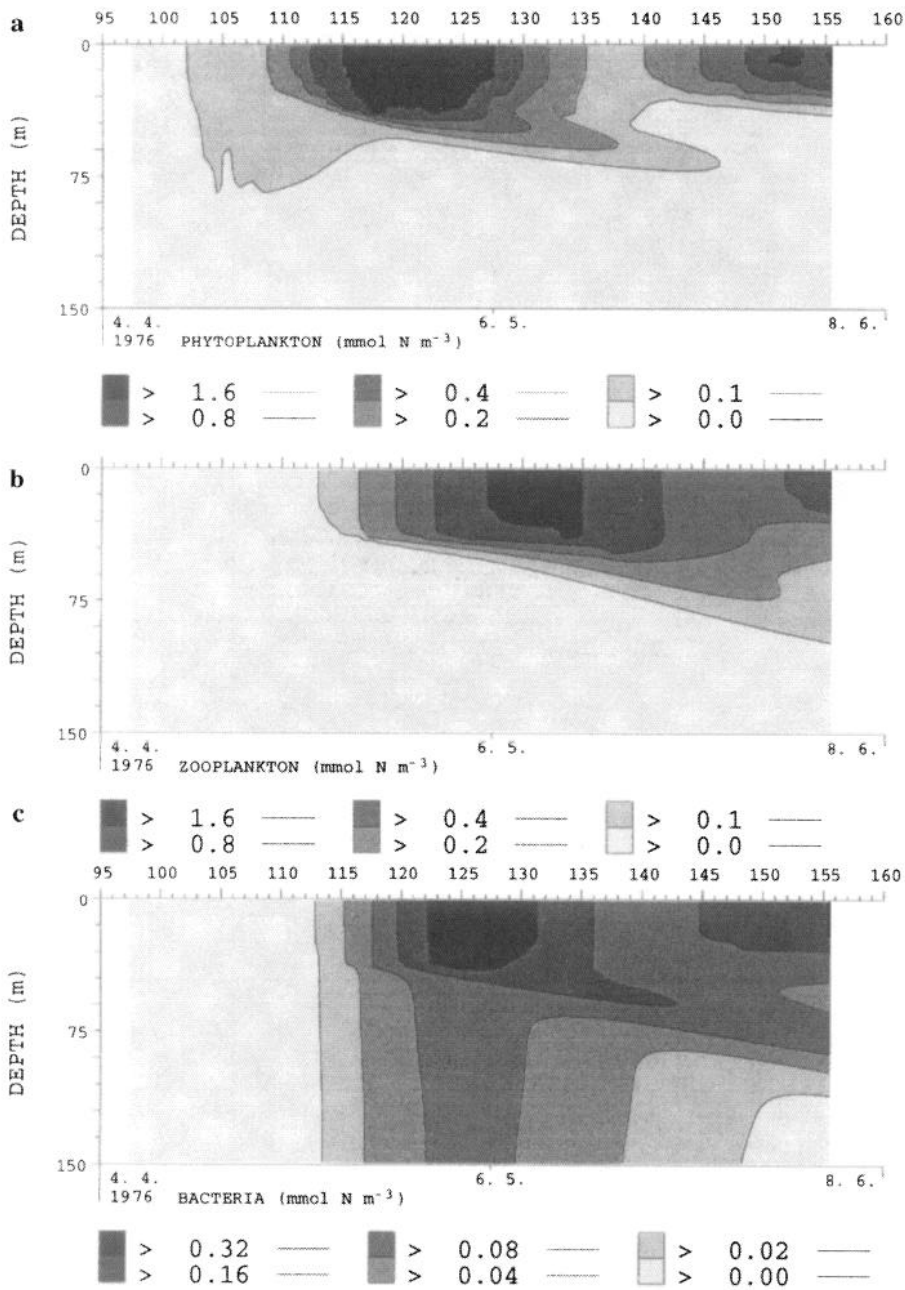

Figure 5. Depth-time contour plots of the seven ecosystem state variables as obtained by the simulation NS: (a) phytoplankton, (b) zooplankton, (c) bacteria, (d) nitrate, (e) ammonium, (f) detritus, (g) labile dissolved organic nitrogen (LDON). Note the different scales.

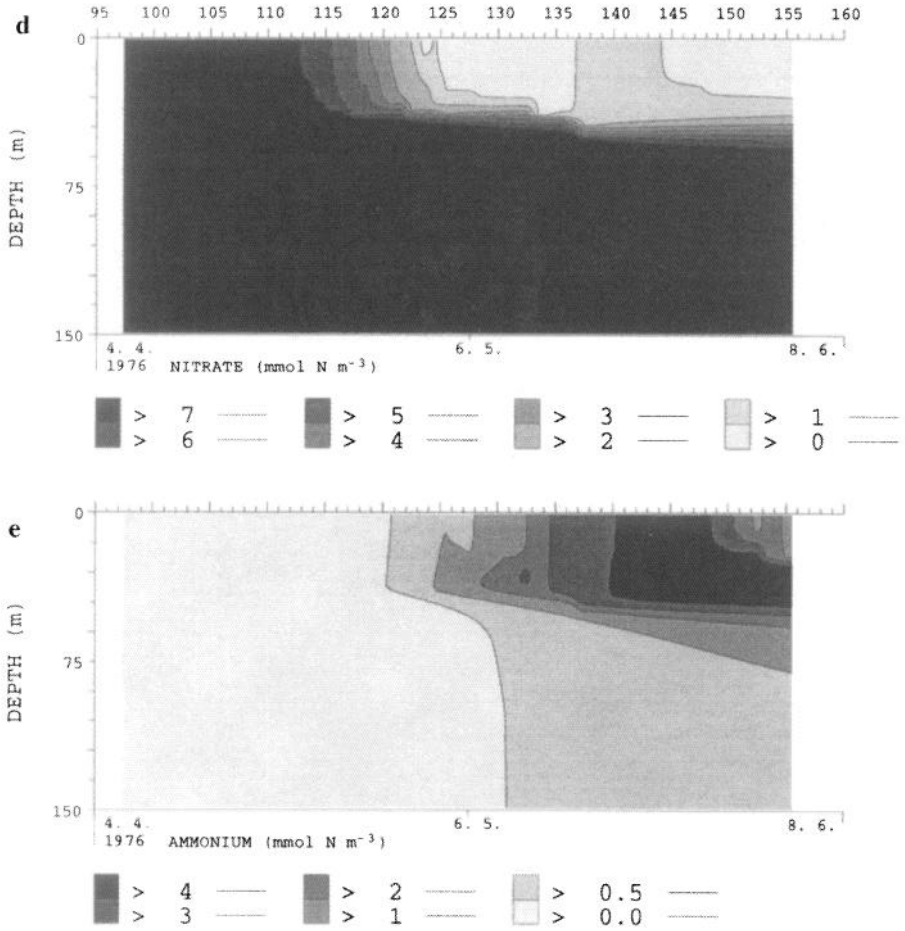

Figure 5. (Continued)

40–50 m. While the zooplankton slowly spreads out into larger depths during the second month of the simulation period, the bacteria are generally abundant in the whole water column, especially at the beginning of May. As Figure 6b shows, herbivorous grazing always dominates, grazing on detritus becomes important after the decline of the first phytoplankton bloom. Grazing on bacteria plays an almost negligible role.

The nitrate pool in the euphotic zone is continuously declining after the beginning of the bloom due to the consumption by phytoplankton (Fig. 5d, 6d). At the same time there is a continuous input due to turbulent diffusion from below; single storm events are clearly to be recognized, especially at days 133 and 137; then the concentration in the upper layer increases markedly (Fig. 5d). The mean depth of the nitracline slowly increases from 40 to 50 m. The ammonium concentration remains rather low and vertically homogeneous during the first three weeks. Then remineralization by zooplankton and—to a much lesser

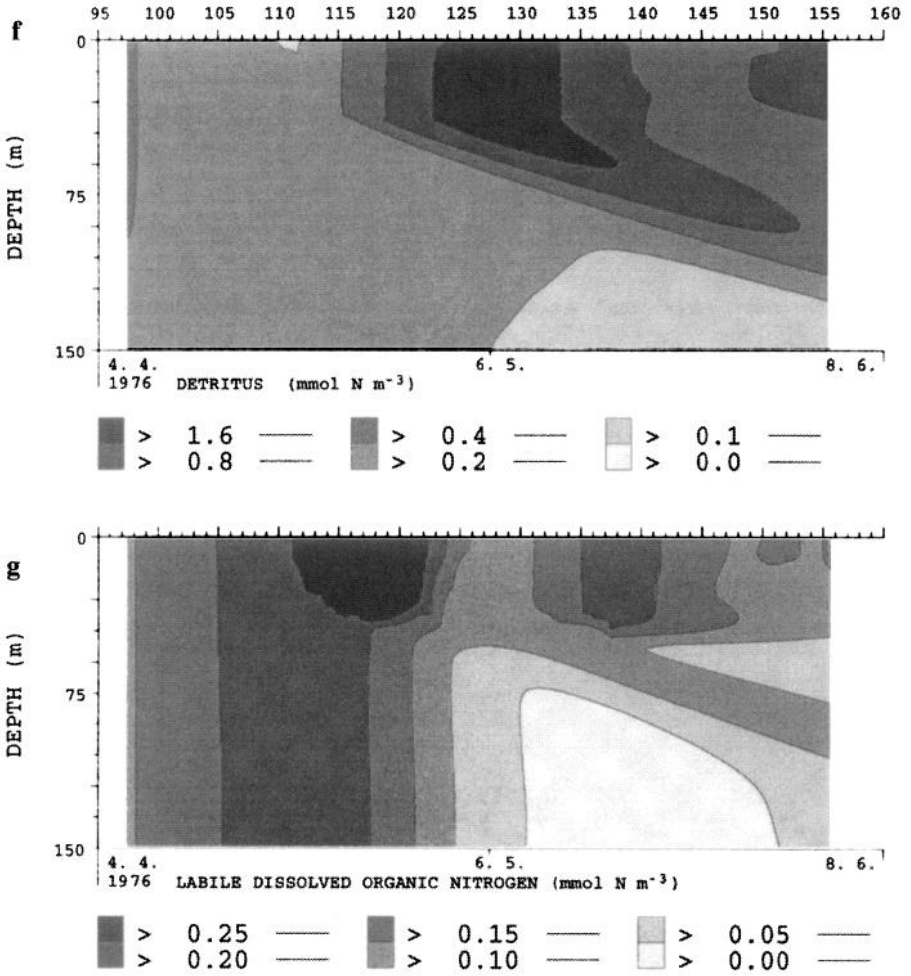

Figure 5. (Continued)

extent—by bacteria over-rides the consumption by phytoplankton, and the ammonium concentration rises, first in the upper layer and then mainly in the region of the thermocline (Fig. 5e, 6e). The relatively high detritus concentration at the beginning of the simulation period quickly diminishes due to sedimentation and biochemical decay to dissolved organic nitrogen (LDON). After about four weeks, when the natural phytoplankton mortality and the production of fecal pellets overcompensate the losses, the detritus pool in the upper layer of the water column reaches a maximum (Fig. 5f, 6f). The concentration of LDON increases during the first three weeks of the simulation period especially in the upper layer reaching a maximum at the end of April before the bacterial growth markedly increases (Fig. 5g, 6g). A second, smaller peak between the days 135–142 is preceding the second phytoplankton bloom. Until the end of April/beginning of May the LDON pool is

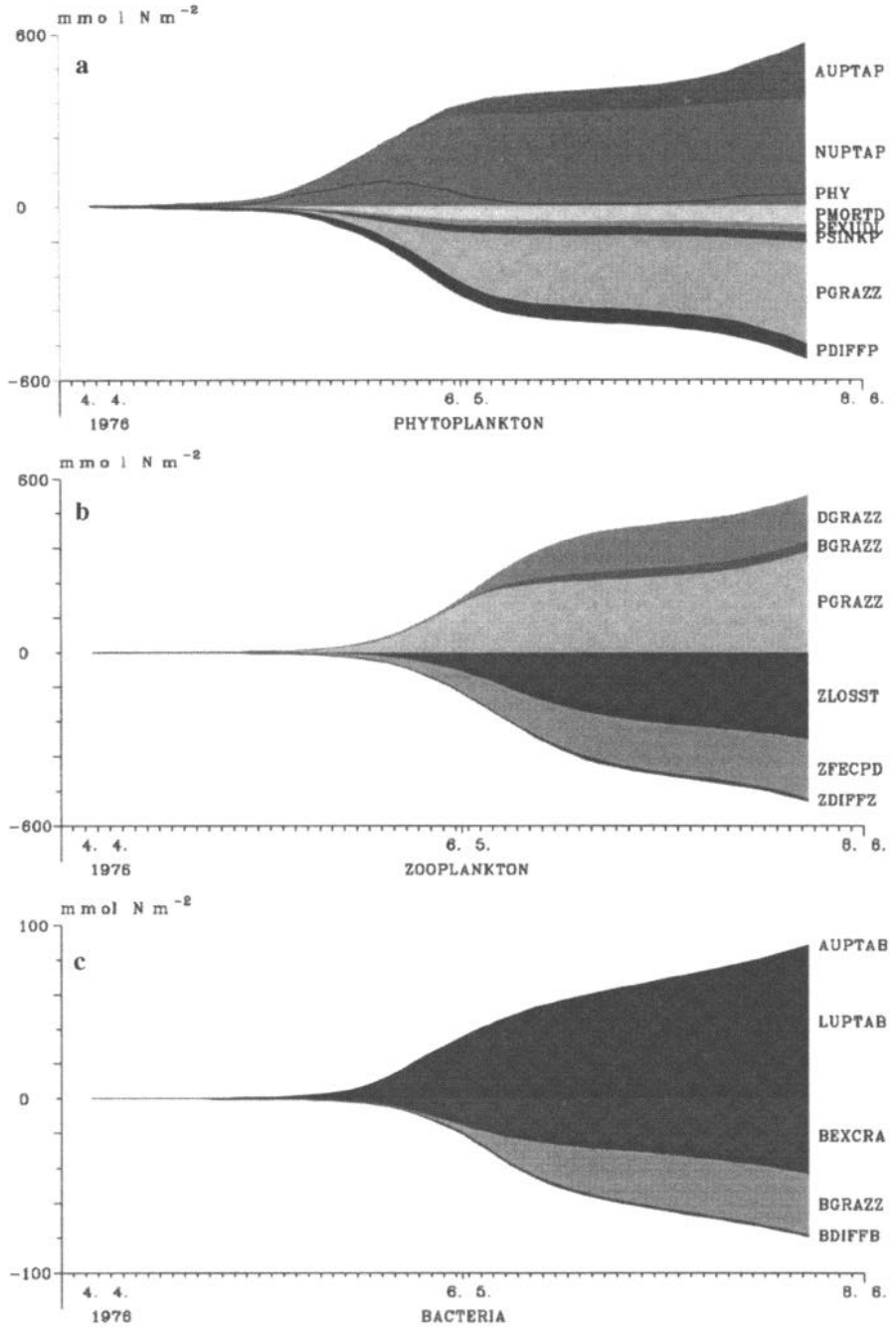

Figure 6. Development of depth-integrated nitrogen fluxes as obtained by the simulation NS (integration depth 30 m): (a) phytoplankton, (b) zooplankton, (c) bacteria, (d) nitrate, (e) ammonium, (f) detritus, (g) labile dissolved organic nitrogen (LDON). The fluxes are time-integrated; the acronyms for the fluxes are explained in Table 4. For comparison the phytoplankton standing stock is shown in (a). Note the different scales.

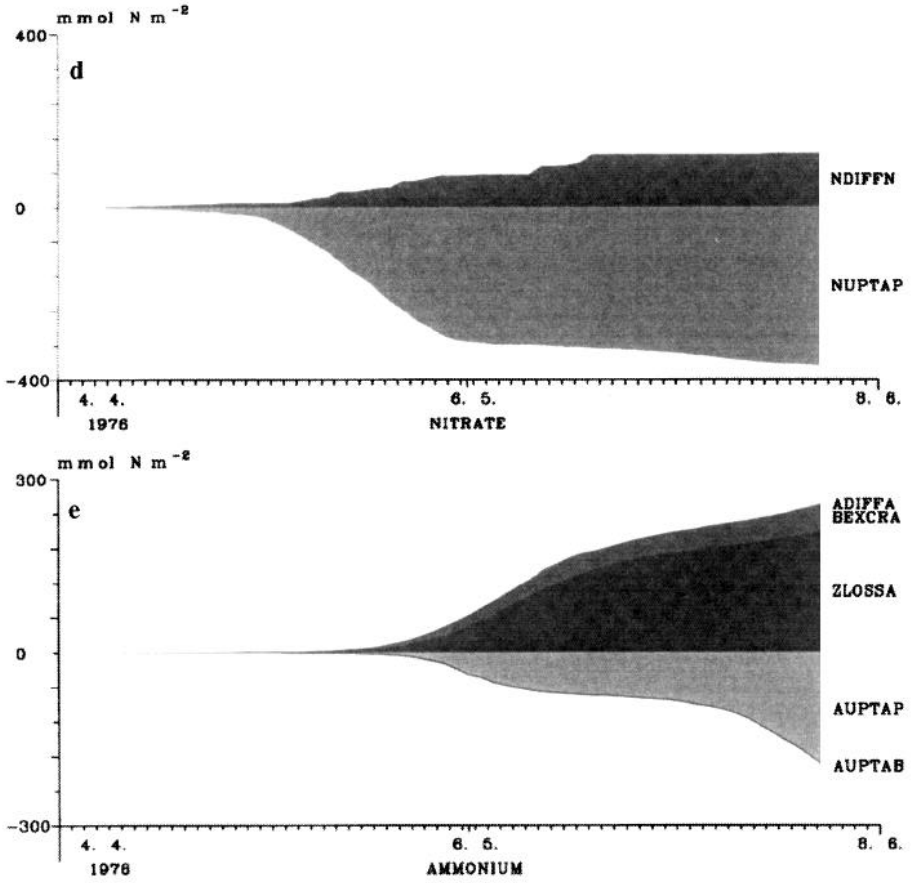

Figure 6. (Continued)

mainly supplied by phytoplankton exudation, afterward the breakdown of detritus and zooplankton excretion are more important sources.

The quantitative results of model run NS are summarized in Tables 4 and 5. As for run NA the temporally and vertically integrated nitrogen fluxes are given for the first month and for the whole simulation period separately (Table 4), the dynamic characteristics are given in Table 5.

The simulations NS and NA differ in the amount and composition of autotrophic production. For the whole simulation period (days 97.0–156.0) the net primary production in run NS is only by 12% higher than in run NA; the new production, however, increased by 43%.

Correspondingly, the mean *f*-ratio is markedly higher: 0.65 compared to 0.51. The differences are even more pronounced, when we look at processes related to heterotrophic activity. The nitrogen uptake by bacteria, i.e. the gross bacterial production, until day 156.0 went down by 61% from 467 mmol N m^{-2} in run NA to only 181 mmol N m^{-2} in run NS.

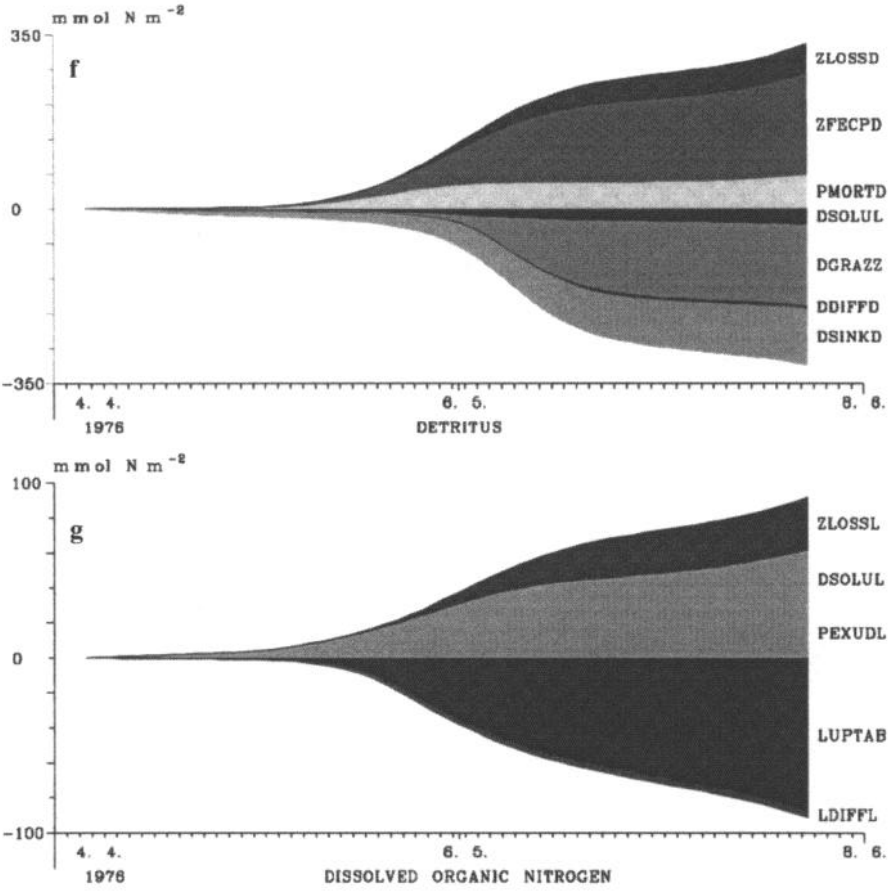

Figure 6. (Continued)

The bacterial net production (total nitrogen uptake minus ammonium excretion) in run NS is even 78% lower. Due to the reduced bacterial standing stock in run NS the composition of the food ingested by zooplankton changed distinctly: whereas in model run NA, 31% of the ingested food was bacteria, in model run NS bacteria make up only 7% of the food. Parallel to this reduction the shares of herbivorous and detritivorous grazing increased. Also the temporal succession in the food composition changed: whereas in run NA, 57% of the grazing on detritus takes place during the first month, in run NS this amounts to only 13%. The total zooplankton grazing is reduced from 922 mmol N m^{-2} in run NA to 802 mmol N m^{-2} in run NS, i.e. by 13%.

As a consequence of the lower heterotrophic activity in run NS also the regeneration of nitrogen in the form of ammonium is markedly reduced. Until day 156.0 the total gross production of ammonium by zooplankton and bacteria amounts to only 431 mmol N m^{-2} in run NS compared to 578 mmol N m^{-2} in run NA. But because in run NS the ammonium

consumption also decreased (208 mmol N m^{-2} compared to 435 mmol N m^{-2} in run NA), the amount of accumulated ammonium is higher in run NS. The lower ammonium consumption in run NS compared to run NA is due to zero ammonium uptake by bacteria and reduced ammonium uptake by phytoplankton. Run NS gives more reasonable results compared to observational findings, especially for the ratio of new and regenerated production and also for the bacterial net production (Table 5). The magnitude of the bacterial growth efficiency and the ratio of LDON exudation by phytoplankton to the LDON uptake by bacteria are more realistic, too.

In spite of the fact that the sinking velocities of detritus are different in the two simulations, the time-integrated PON sedimentation fluxes are nearly the same. The higher sinking velocity of detritus in run NA is compensated by the lower concentration due to larger losses by breakdown and detritivorous grazing within the first month. In both simulations we observe an overestimation of the export flux to the bottom during the first month and a slight underestimation during the second month. This is an effect of using constant sinking velocities whereas in reality the sinking velocity averaged over the different particles presumably varies in time.

ii. Comparison of run NS with observations: Primary production. Comparing the model result for net primary production with the result of ^{14}C measurements by Weigel and Hagmeier (1978) and (Radach *et al.,* 1984) one notices that besides the time-integrated value also the evolution in time and the daily variability are reproduced (Fig. 7a). There are, however, some noticeable differences. The simulated primary production before the beginning of the bloom at day 110 is lower than observed, during the bloom the simulated production curve lies above the observed one. The secondary rise of primary production is delayed in the simulation by a few days. The low production observed before the onset of the bloom and the increase of production after day 138 were presumably caused by small autotroph flagellates (Wandschneider, 1983) whose growth parameter are probably different from those chosen in the simulation which are more typical for large phytoplankton. Considering the fact that the ^{14}C method is supposed to measure something between gross and net primary production one could argue that model run NS overestimates net primary production. On the other hand, for the period 19 April–1 May (days 110–122) Weichart (1980) determined a mean daily net primary production of 2.0 g C m^{-2} d^{-1} which is definitely higher than the values measured by Weigel and Hagmeier (1978) but is quite near to what we find in model run NS.

Nitrate. The observed decline of the nitrate concentration in the euphotic zone (Brockmann *et al.,* 1983) is reproduced rather well by model run NS (see Fig. 4b) with the exception that the slow decrease of the nitrate concentration before day 110 is not to be found in the simulation. This delay in the decrease of nitrate corresponds with the misfit in the production curve before day 110 and is the reason for the time lag of about 4 days between the simulated and the measured nitrate curve after day 110. The increase of nitrate

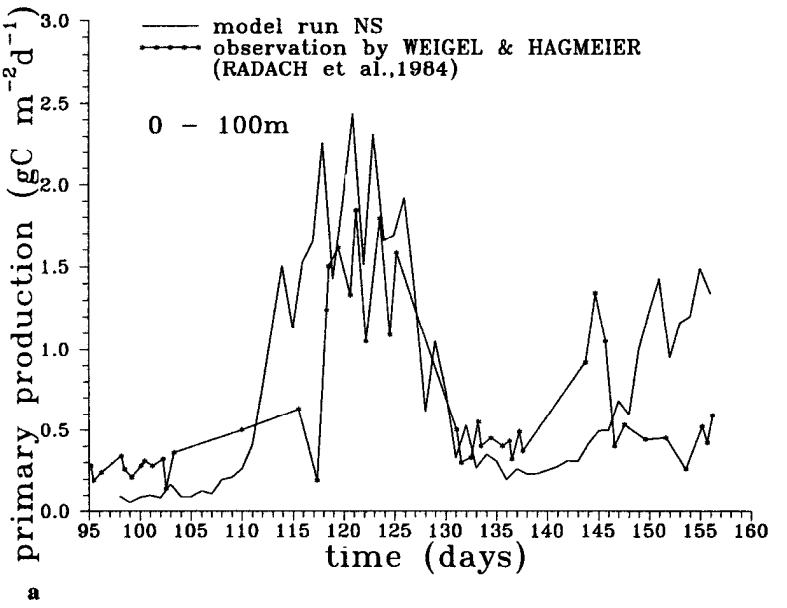

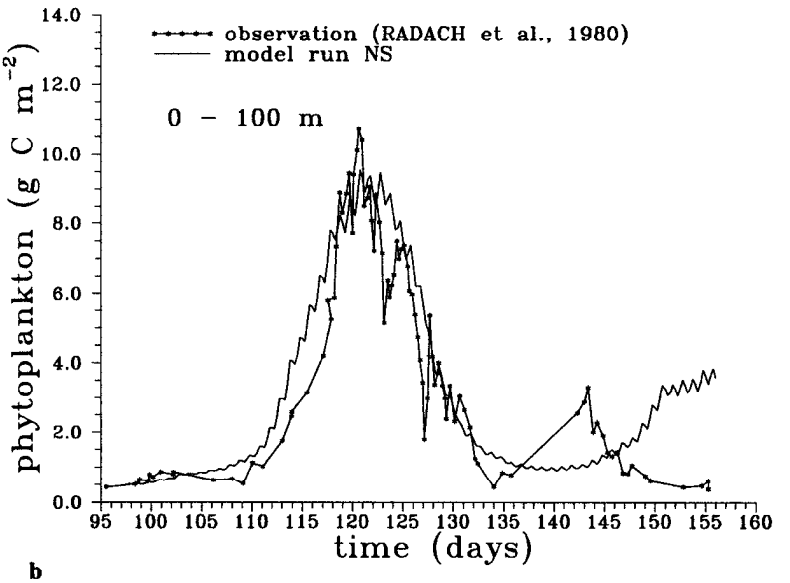

Figure 7. (a) Primary production during FLEX '76—comparison of simulation NS and observation (Radach *et al.*, 1984); (b) phytoplankton standing stock in the upper 100 m during FLEX '76—comparison of simulation NS with observation (Radach *et al.*, 1980).

concentration in the upper layer between days 127 and 132, not to be seen in the simulation, must have been caused by horizontal advection (as discussed above), whereas the steep rises at days 133 and 137 are due to the turbulent entrainment of nitrate from below during heavy storms (cf. Fig. 1a).

Phytoplankton. The comparison of simulated and observed development of the phytoplankton standing stock in the upper 100 m is shown in Figure 7b. The observational curve was obtained from photometric chlorophyll measurements using a Chl *a*/C-ratio of 20 (Radach *et al.*, 1980). The result of simulation NS fits the observation quite well; the onset of the secondary, minor bloom, however, is delayed in correspondence with the delay in the primary production.

PON. The concentration of PON in the upper layer (0–50 m) is shown in Figure 8a. The observed PON concentration (Hammer *et al.*, 1983) refers to the upper layer above the main thermocline, which had a time-varying depth, the mean value of which was about 50 m. The simulated PON concentration was obtained by averaging over a constant depth of 50 m. The steep increase by about 5 mmol N m^{-3} after day 110 is reproduced by the simulation, but with a time lag of 3–5 days. This delay may be partly caused by an overestimation of the losses of the model detritus pool, partly by a too low production of detritus during the first 14 days. The PON concentration averaged over the whole water depth as obtained from the simulation is also shown in Figure 8a. It exhibits the same delay of the maximum in comparison to the observation. Additionally the concentrations are generally too low. Taking two results together, it is obvious that the amount of PON in the lower layer is somewhat underestimated by the simulation.

Ammonium. The mean ammonium concentrations in the upper layer (0–50 m) and in the whole water column are shown in Figure 8b. Evidently, model run NS reproduces the tendency of increasing NH_4 concentrations during the two months of the spring bloom. Both simulated ammonium curves do not exhibit the rather sharp peaks observed at days 112 and 118, respectively. The ammonium concentration in the upper 50 m becomes much too high (with a maximum of about 4.5 mmol N m^{-3}) after day 135. The mean ammonium concentrations in the upper layer observed during the last phase of FLEX '76 (22 May–5 June) were in the range 2–3 mmol N m^{-3} (Eberlein *et al.*, 1980). If we compare this discrepancy with the rather good accordance between simulated and observed mean ammonium concentration in the whole water column (Fig. 8b), it is obvious that the ammonium concentrations in the lower layer are underestimated to the advantage of those in the upper layer. This may be caused in part by the too strict confinement of the model zooplankton within the upper layer whereas in reality after the middle of May (day 140) the zooplankton (at least the copepods) was beginning to vertically migrate, excreting ammonium also into the lower layers (Krause and Radach, 1989). Additionally, delay of the second, minor bloom in the simulation favors the too strong accumulation of NH_4 in the

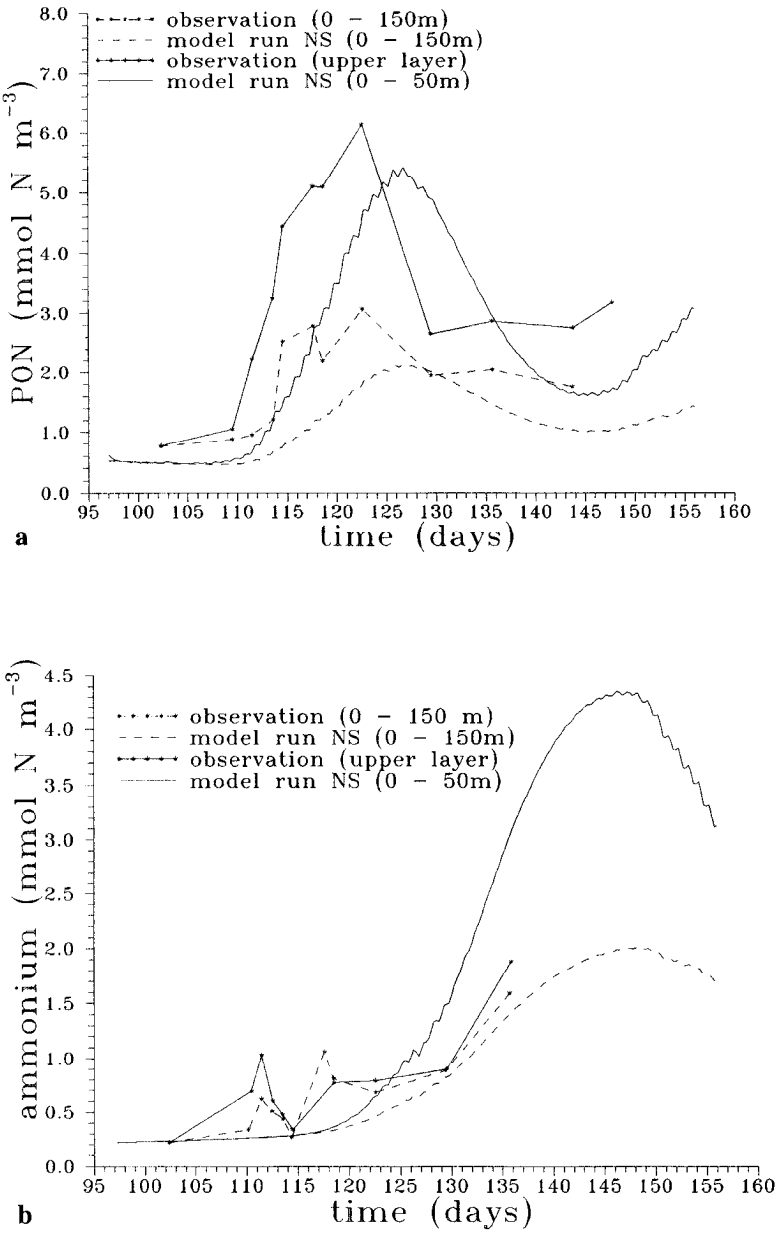

Figure 8. (a) Depth-averaged PON concentration during FLEX '76 for the upper 50 m and for the whole water column; (b) depth-averaged ammonium concentration for the upper 50 m and for the whole water column. Comparison of model run NS with observation (Hammer *et al.*, 1983).

upper layer in the late spring. By including nitrification, it is possible to reduce the amount of ammonium accumulated in the upper layer, but at the same time also in the lower layer, so that the average concentration in the total water column becomes too low. This point cannot be clarified, however, because a certain advective input of ammonium during the observation period, especially after day 128.0, cannot be ruled out.

Zooplankton. In Figure 9a the standing stock of the model zooplankton in the upper 100 m is shown and compared with the development of the biomass of *C. finmarchicus.* Obviously the model zooplankton develops differently than *C. finmarchicus:* the pronounced maximum in the model zooplankton standing stock around day 132 represents a biomass more than twice as high as that observed for *C. finmarchicus.* One has to take into account, however, that the model zooplankton comprises meso- and microzooplankton and that *C. finmarchicus* makes up only one part (though the dominant one) of the observed herbivorous mesozooplankton. We conclude that if the decline of the phytoplankton is due to zooplankton grazing, then there must have been strong herbivorous grazing by microzooplankton during that period. For the whole simulation period the total amount of ingested food of 805 mmol N m^{-2} or 64.0 g C m^{-2}, respectively, falls into the range of the most reliable estimates of mesozooplankton grazing according to Radach *et al.* (1984). The results for the first month, however, differ widely: the total grazing in the simulation amounts to 22.5 g C m^{-2} (82% of which are herbivorous grazing), whereas the estimates from observations range only from 5 to 10 g C m^{-2}. Figure 9b shows the different temporal course of the cumulated grazing for the model zooplankton and for *C. finmarchicus.* From a model study on the dynamics of phytoplankton and *C. finmarchicus* during FLEX '76 also Carlotti and Radach (1996) conclude that microzooplankton must have served to graze down the phytoplankton bloom and to provide food for the copepods.

LDON. The mean LDON concentration in the upper 50 m resulting from simulation NS is compared in Figure 10a with the mean concentrations of dissolved free amino acids (DFAA) in the upper layer observed during FLEX '76 (Hammer *et al.,* 1983). The DFAA peak during the exponential growth phase of phytoplankton is reproduced in the simulated LDON curve though slightly shifted and broadened. Also the peak in the DFAA concentration averaged over the total water depth is mirrored by the model result for LDON (Fig. 10a). The early rise of the simulated LDON concentration before day 110 is presumably caused by a certain overestimation of the biochemical decay of detritus during that period.

Bacteria. The comparison of modeled bacteria is hampered by the very limited observations. General statements about bacterial activity are well met by simulation NS as can be seen in Table 5. Typically the bacterial production is in the order of 20–30% of net primary production (Cole *et al.,* 1988); the growth efficiency of bacteria is about 50%, and not more than 20% of the organic matter requirements of bacterioplankton is supplied by phytoplank-

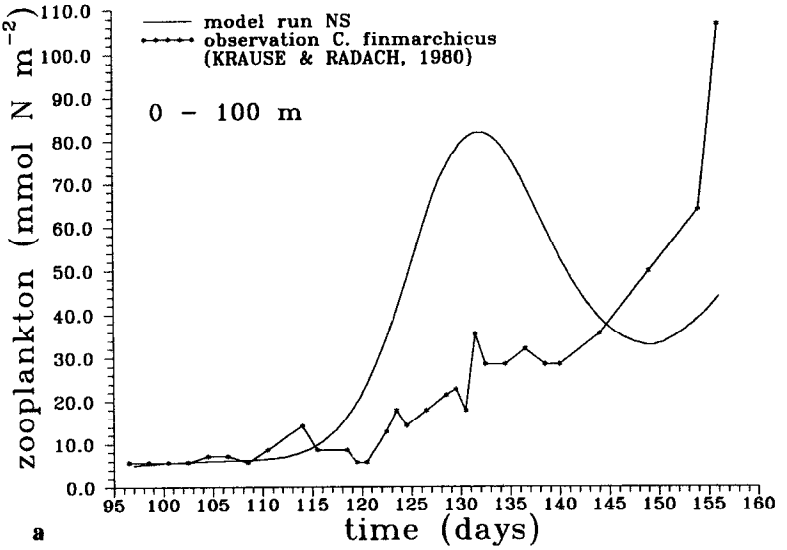

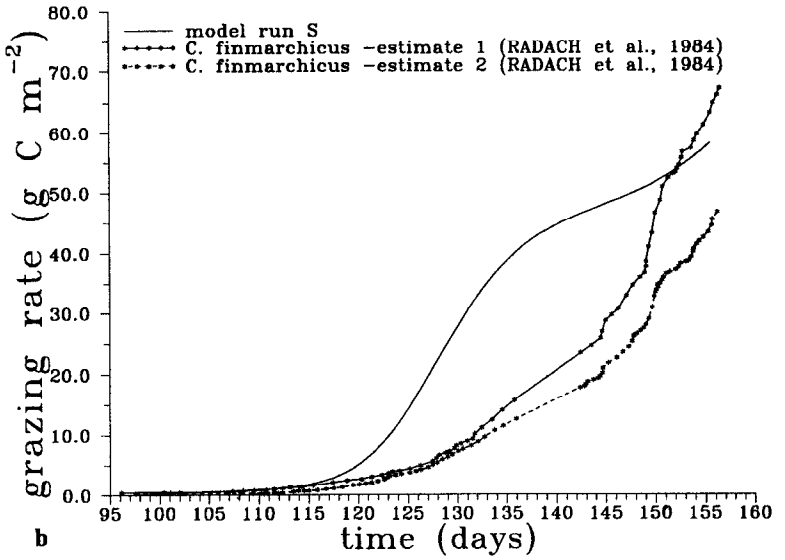

Figure 9. (a) Zooplankton standing stock in the upper 100 m as obtained from simulation NS compared with the development of the biomass of *C. finmarchicus* as observed during FLEX '76 (Krause and Radach, 1980); (b) cumulative total grazing of model zooplankton within the upper 100 m as obtained from simulation NS compared with different estimates of cumulative grazing of *C. finmarchicus* during FLEX '76 (Radach *et al.*, 1984)

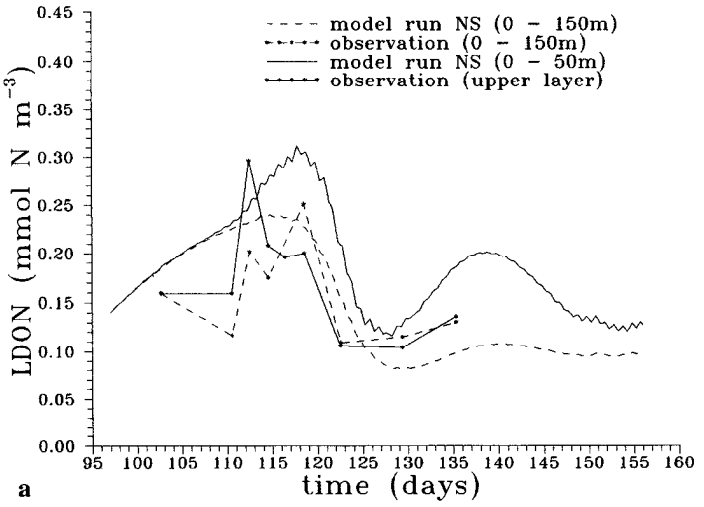

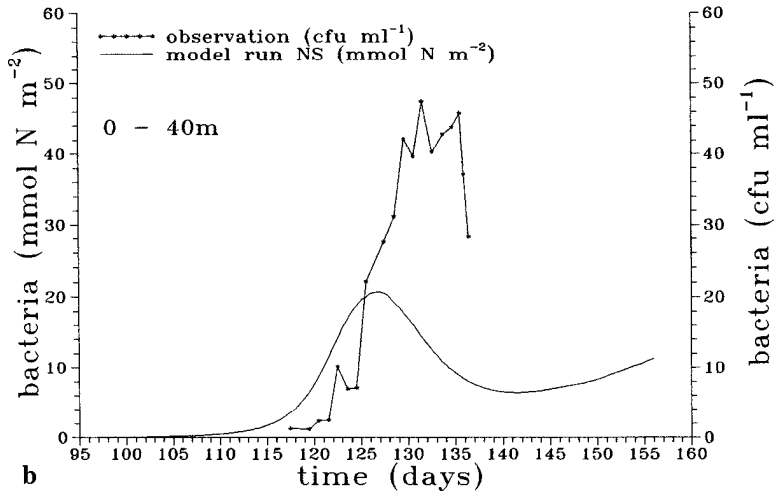

Figure 10. (a) Depth-averaged concentration of labile dissolved organic nitrogen (LDON) for the upper 50 m and for the whole water column as obtained from simulation NS compared with the depth-averaged concentration of dissolved free amino acids as observed during FLEX '76 (Hammer *et al.*, 1983); (b) the bacterial biomass integrated over the euphotic zone (in mmol N m^{-2}) as obtained from simulation NS compared with the mean bacterial numbers in the upper 40 m (in cfu ml^{-1}) as observed during FLEX '76 (Hentzschel, 1980).

ton exudation (Billen *et al.,* 1990). During FLEX '76 the bacterial standing stock was measured using the plate (or colony) count technique without converting the results into biomass values (Hentzschel, 1980). In Figure 10b the bacterial biomass integrated over the euphotic zone (0–30 m) as obtained from the simulation NS is shown together with the observed numbers of bacteria (in cfu ml^{-1}) averaged over the upper 40 m (Wandschneider, 1983). A sharp increase of the observed standing stock of bacteria occurs after day 122, i.e. after the exponential growth phase of the phytoplankton, with a maximum at day 132 when the phytoplankton bloom nearly had vanished. The simulation reproduces the strong increase and the formation of a maximum of the bacterial biomass, though a few days too early. Assuming the relations 1 cfu $\approx 10^3$ cells (Billen *et al.,* 1990) and 1 cell = 2 10^{-14} g C (Ducklow *et al.,* 1993) and a bacterial C/N ratio of 5 one obtains the equivalence 50 cfu ml^{-1} = 0.02 mmol N m^{-3}. Integrating over the euphotic zone yields 0.6 mmol N m^{-2}, a value 25 times less than the peak value in the simulation (15 mmol N m^{-2}). However, the conversion of bacterial plate count numbers into biomass is a highly uncertain procedure. In any case the bacterial biomass is negligibly small compared to that of phytoplankton, zooplankton and detritus.

Summarizing, it is possible to reproduce net primary production and sedimentation flux of particulate organic matter during the main production period in the northern North Sea rather well when using the oceanic parameter set NA and the nutrient uptake formulation according to Wroblewski (1977). The simulation NA, however, fails with respect to the ratio of new and regenerated primary production and to the order of magnitude of bacterial production. New production is underestimated, whereas regenerated production, bacterial production and zooplankton grazing on bacteria obviously are overestimated. Because the latter processes are immediately connected with the regeneration of nitrogen, considerable deviations from reality will be likely to occur when simulating a full annual cycle of the plankton dynamics in the northern North Sea.

The modified parameter set NS and the limitation function according to O'Neill *et al.* (1989) (with higher affinity for nitrate than for ammonium) results in a simulation showing good overall accordance with the observations. Primary production and standing stock of phytoplankton during the diatom-dominated bloom are well described. The secondary, flagellate-dominated phytoplankton peak occurs some days too late in the simulation. Another problem concerns the zooplankton development. In the simulation the breakdown of the first bloom is caused by strong herbivorous grazing which is far beyond the estimates for herbivorous grazing obtained from observations of mesozooplankton. This suggests a strong development of herbivorous microzooplankton during the bloom. An alternative explanation—a breakdown of the main bloom due to depletion of phosphate—was offered earlier by Radach *et al.* (1984). Further, in the simulation we find a certain underestimation of the amount of PON in the whole water column, especially in the lower layer. Presumably two reasons may be responsible for this discrepancy. Firstly, there may have been some 'hidden' lateral input of nutrients by advection, which was immediately converted into PON. Secondly, the temporal dynamics of sinking of particulate matter are certainly not

sufficiently well described by constant sinking velocities for phytoplankton and detritus. This is suggested by the fact, that the simulated sedimentation flux during the first month with 5% of the net primary production is overestimated, whereas for the whole simulation period this flux is at the lower end of the observed range. During the second month the simulation produces not enough ammonium in the lower water column and too much in the upper layer. This may be partly caused by the too strict confinement of the zooplankton to the upper layer.

iii. Budget of nitrogen fluxes. The results of simulation NS of the spring bloom at the FLEX '76 central station for the period with low advective influence (days 97.0–128.0) will be presented now in terms of a nitrogen budget. In Figure 11a the intercompartmental fluxes and the temporal changes in the stocks (denoted as D) within the euphotic zone (0–30 m) and in the water column below (30–150 m) as well as the vertical transports are shown. The model compartments phytoplankton, zooplankton, bacteria and detritus are taken together as PON ('particulate organic nitrogen'). The term 'release' summarizes LDON excretion by zooplankton, exudation by phytoplankton and decay of detritus to LDON. The term 'regeneration' denotes the excretion of ammonium by zooplankton and bacteria.

From Figure 11a the simulated spring bloom dynamics in the northern North Sea can be characterized as follows:

- Whereas 98% of the primary production take place within the euphotic zone, the regeneration of nitrogen occurs in the whole water column. The latter amounts to 67 mmol N m^{-2} in the euphotic zone and 49 mmol N m^{-2} in the water column below; i.e., in volumetric units the regeneration of nitrogen is stronger in the upper 30 m.

- The net consumption of dissolved nitrogen (net uptake of nitrate, ammonium and LDON) amounts to 250 mmol N m^{-2} for the whole water column. After conversion into particulate organic nitrogen (PON) only 7% of this amount (18 mmol N m^{-2}) are exported to the bottom during this month of major productivity whereas the overwhelming part (232 mmol N m^{-2}) is intermediately accumulated in the water column.

- The nitrogen equivalent of the net primary production in the euphotic zone (350 mmol N m^{-2}) is delivered to about 69% by mineral nutrients (nitrate) initially available in the euphotic zone, to 20% by turbulent diffusive import of nitrate from the water column below and to further 11% by nutrient regeneration within the euphotic zone.

- The fluxes between the PON and the LDON pools are considerable; the total release of LDON amounts e.g. to 69 mmol N m^{-2}. Due to the high turnover rates of LDON the contents of the LDON pools in the euphotic zone and in the water column below are, however, almost unaltered after one month.

- The PON export out of the euphotic zone amounts to 39% of new production. This shows that the commonly assumed identity of export production and new production

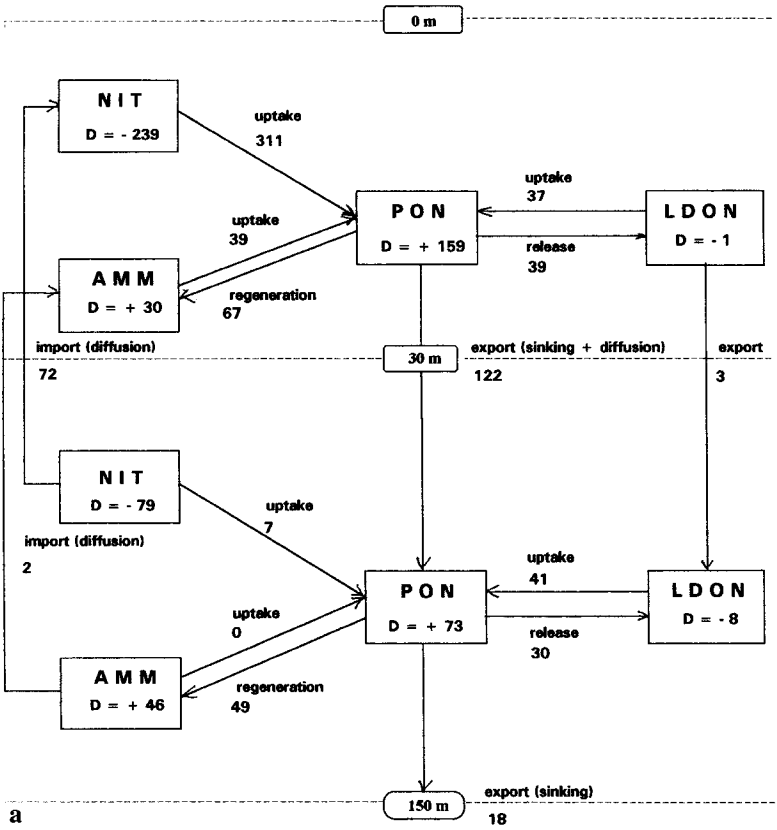

Figure 11. Budget of nitrogen fluxes (in mmol N m^{-2}) and changes in standing stocks (D, in mmol N m^{-2} (time span)$^{-1}$) for the simulation period 7 April, 0 h − 7 May, 24 h, during FLEX '76: (a) euphotic zone and lower layer separated, (b) for the whole water column. NIT nitrate, AMM ammonium, PON particulate organic matter (phytoplankton, zooplankton, detritus, bacteria), LDON labile dissolved organic nitrogen. The numbers after the slash in (b) are deduced from observations.

is not justified on time scales in the order of one month because of the high 'storage capacity' of the system; 51% of the new production are stored as PON and 10% as ammonium. Integrated over the whole simulation period of two months, 56% of the new production are exported out of the euphotic zone.

The nitrogen budget for the whole water column without separating the euphotic zone from the deeper layer allows the comparison with budget data derived from observation (Fig. 11b). The order of magnitude for new and export production is well met by the simulation. Moreover, also the changes in the amounts of PON, ammonium and LDON are approximately reproduced by the simulation. However, observational data also show that the sum of those changes plus the amount of PON exported to the bottom (336 mmol N

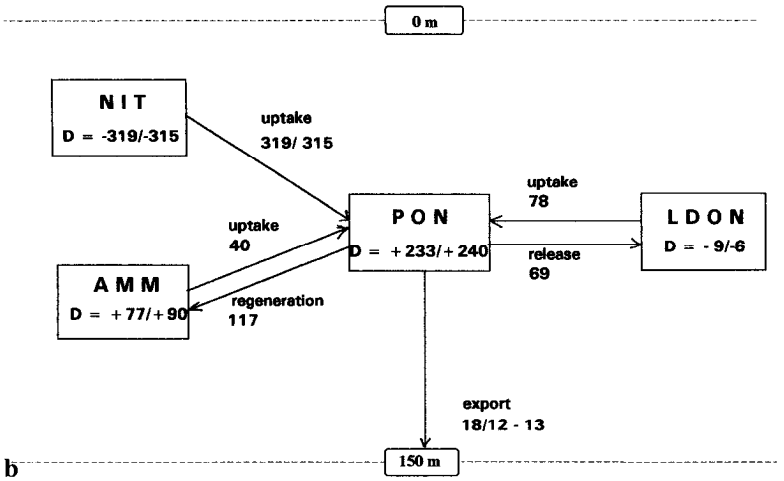

Figure 11. (Continued)

m^{-2}) is somewhat larger than the observed decrease of the nitrate pool (-315 mmol N m^{-2}), i.e. the nitrogen budget obtained from observations is not exactly closed. The difference of 21 mmol N m^{-2} can probably be explained by advective import of nitrate subsequently converted into PON and ammonium, respectively. If this interpretation is correct, then during the time period characterized above as 'weakly influenced by advection' about 7% of the new production were fueled by horizontally advected nitrate.

iv. Vertical particle flux. How does the vertical particle flux in the water column vary with depth and how is this flux related to primary production in the euphotic zone, especially how much of the overlying production leaves the euphotic zone and how much reaches the bottom? The answer will depend on several factors, e.g. on the ratio between the average velocity of the sinking material and the regeneration rate of the ecosystem within and below the euphotic zone. Moreover, the relation between primary production and particle flux depends essentially on the time scale over which the correlation is traced. To illustrate this, the daily sinking PON fluxes out of the euphotic zone are correlated with the daily net primary production values, both obtained from simulation NS (Fig. 13a). Obviously, there is no linear relation. The trajectory of the system in the two-dimensional phase space is rather a polygon. Such a curve is characteristic for processes exhibiting a phase shift. When using 10-days mean values the original polygon is still roughly reproduced, whereas 20-day mean values yield a linear relation and 30-day mean values even feign a negative correlation. This clearly shows that one has to be careful when interpreting averaged particle flux data in relation to averaged primary production data.

The simulated vertical flux of particulate organic nitrogen is composed of (a) sinking fluxes of phytoplankton and detritus and (b) vertical transport due to turbulent diffusion of phytoplankton, detritus, zooplankton and bacteria. The share of the turbulent diffusive flux

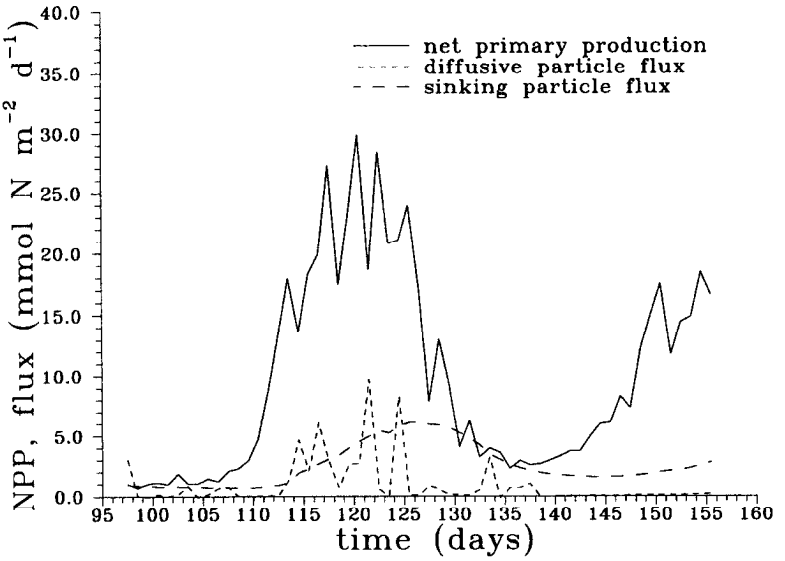

Figure 12. Daily particle fluxes out of the euphotic zone due to sinking and due to turbulent diffusion in comparison with the daily net primary production (NPP).

generally decreases with depth. The actual depth dependence is, however, determined by the existing gradients, which themselves are influenced by the sinking and mixing processes. For a given depth the ratio between the fluxes due to sinking and due to turbulent mixing depends on the hydrodynamic situation in the water column and therefore on the time range regarded. Thus, in the simulation the total PON flux over the depth of 30 m until day 128.0 amounts to 122 mmol N m^{-2}, which corresponds to 35% of net primary production in the same period; 40% of this export flux are due to turbulent diffusion. Until day 156.0 the total PON export out of the euphotic zone amounts to 204 mmol N m^{-2} corresponding to 36% of the net primary production during that period. The share of turbulent diffusive export, however, has decreased to only 28% of the total flux. The reason is that the storms between days 113 and 125 occur, when a high concentration of particulate organic matter exists in the upper layer, and therefore cause high turbulent transports, while the even stronger storms at days 133 and 137 meet a fairly uniform depth profile of POM and consequently the vertical diffusive transport of particulate matter is relatively low (Fig. 12). The storms after day 140 are not able to generate high turbulent mixing because the stratification of the water column is already very stable (cf. Fig. 2).

The depth dependence of the ratio of the total vertical particle flux to net primary production obtained from the simulation NS after integrating over the whole simulation period is shown in Figure 13b. Also shown are graphs obtained from different empirical expressions describing the vertical export flux Φ in dependence on depth z (with $z \geq$ depth of the euphotic zone) and on net primary production PP in the euphotic zone:

$$\Phi(z) = 20/z\ \mathrm{PP} \quad \text{(Berger } et\ al.\text{, 1988)}, \tag{1}$$

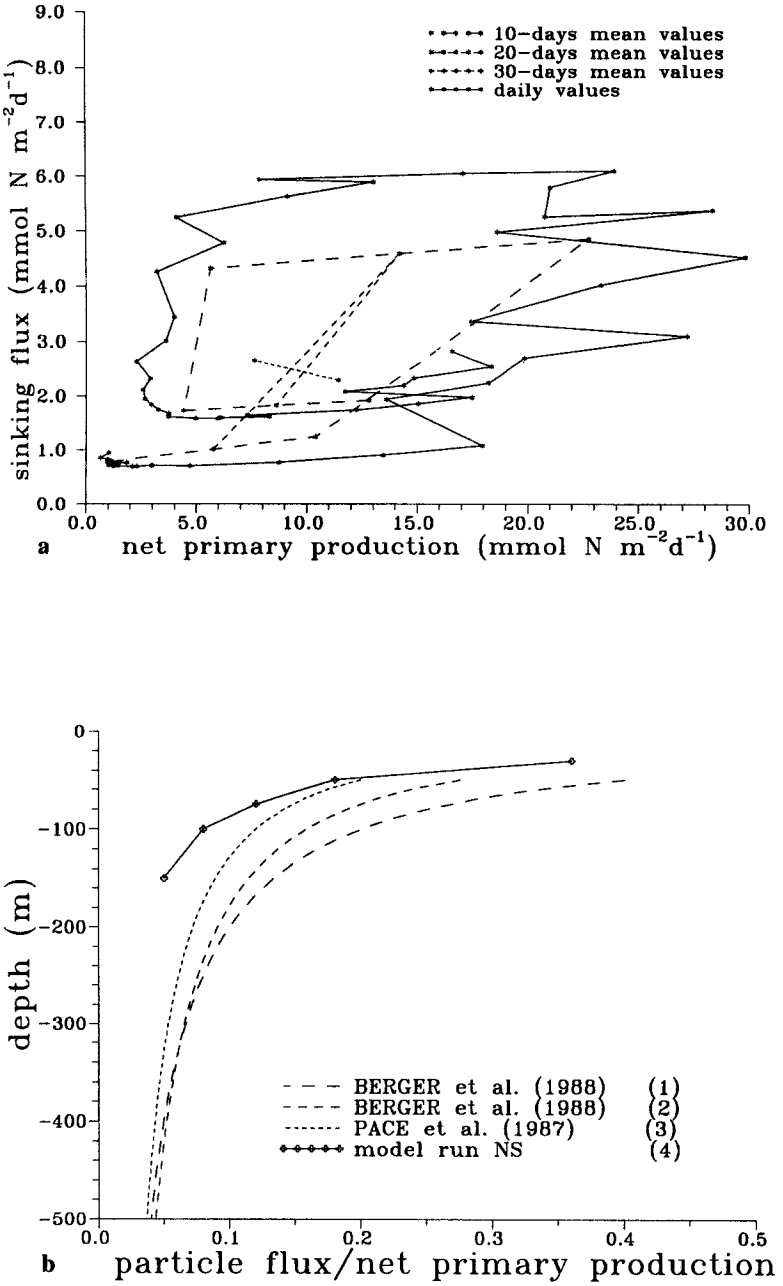

Figure 13. (a) Correlation between the PON export flux out of the euphotic zone and net primary production as obtained from simulation NS for different averaging intervals; (b) depth dependence of the total vertical PON flux (due to sinking and turbulent diffusion) normalized to net primary production NPP in the euphotic zone as obtained from simulation NS (full line with dots). The dashed curves represent different empirical expressions for the depth dependence of the ratio PON flux/NPP (Pace et al., 1987; Berger *et al.*, 1988).

$$\Phi(z) = 6.3/z^{0.8}\ \mathrm{PP} \quad \text{(Berger } et\ al.\text{, 1988)}, \tag{2}$$

$$\Phi(z) = 3.523/z^{0.734}\ \mathrm{PP} \quad \text{(Pace } et\ al.\text{, 1987)}. \tag{3}$$

For the bottom of the euphotic zone the ratio Φ/PP falls into the range given by the empirical expressions (2) and (3) given by Berger *et al.* and Pace *et al.,* respectively. At greater depths we observe a much stronger decrease in simulated ratio. Note, however, that the expressions (1)–(3) relate to the flux of particulate organic carbon, whereas the model yields the flux of particulate organic nitrogen. Only if the C/N ratio does not vary with depth the vertical PON flux can be described by the same formulae; otherwise the depth dependence of the C/N ratio has to be taken into account. During FLEX '76 Davies and Payne (1984) observed an increase of the C/N ratio from about 6.6 (Redfield ratio) within the euphotic zone to values in the range 9 to 18 near the bottom at 150 m depth. A similar tendency—though not so strong—was found by Martin *et al.* (1987) in the VERTEX flux investigations in the north-east Pacific and by Martin *et al.* (1993) in the northeastern Atlantic. This shift of the C/N ratio must be caused by preferential regeneration of nitrogen in deeper layers.

A least-square fit of the dots in Figure 13b yields the expression

$$\Phi_N(z) = 22.1/z^{1.22}\ \mathrm{PP}_N.$$

If we assume the validity of the expression (2) given by Berger *et al.* (1988) also for the FLEX '76 situation then the increase of the C/N ratio r with depth obeys the relation:

$$r(z) = 0.28/z^{0.42}\ r_0,$$

With the Redfield ratio $r_0 = 6.625$ one obtains a C/N ratio of $r = 15$ at the bottom ($z = -150$ m), which is indeed the range of the values observed during FLEX '76.

5. Conclusions

We developed a one-dimensional, physical-biological water column model of the pelagic ecosystem and applied it to the spring bloom in the northern North Sea making use of the rather comprehensive data set obtained during the Fladenground experiment FLEX '76. The model consists of a physical upper layer model and an ecosystem model of the lower trophic levels in the pelagic. The physical submodel is a second-order turbulence closure model of level 2 type developed by Mellor and Yamada (1974, 1982). The biological submodel is a depth-resolved version of the nitrogen flux model proposed by Fasham *et al.* (1990).

The physical submodel driven with realistic meteorological and radiation data describes the development of thermal stratification at the FLEX '76 central station (58° 55′ N, 0° 32′ E) during the spring very satisfactorily. The observed SST and the mixed layer depth could be reproduced very well. Toward the end of the simulation period the width of the thermocline is slightly underestimated.

We investigated, whether the biological model configuration (including the nutrient

uptake formulation and the parameter values) used by Fasham *et al.* (1993) for basin-scale simulations of the pelagic ecosystem in the North Atlantic is also able to describe the evolution of the North Sea ecosystem during a spring bloom. We found that the model is not transferable without modifying a series of important ecological model parameters. If we use the original parameters chosen for the North Atlantic the resulting net primary production and sedimentation flux comes out in the right order of magnitude, but the ratio between new and regenerated production is unrealistic because the uptake of ammonium and the bacterial production are overestimated. Using a parameter set adapted to the North Sea ecosystem we obtain a realistic overall description of the North Sea ecosystem.

We investigated the nutrient inhibition by using different formulations for the simultaneous uptake of the inorganic nutrients nitrate and ammonium by phytoplankton. We propose to use the parameterization deduced from the model of substitutable resources (O'Neill *et al.,* 1989) which proved to be more general and more flexible than the very special and restricted parameterization by Wroblewski (1977). An important result of our simulation is that a higher affinity of phytoplankton for nitrate than for ammonium has to be assumed to reproduce the observational data.

Using this uptake parameterization and the modified parameter set NS we were able to hindcast successfully the onset, duration, magnitude and daily variability of the net primary production, the magnitude of the PON export flux to the sea bottom, the bacterial production and the nitrogen regeneration within the water column. From the results of the simulation we calculated a nitrogen budget summarizing the changes of standing stocks and the intercompartmental fluxes within both, the euphotic and the aphotic zones, as well as between them. One discrepancy between model output and observation is that during the whole simulation period the total amount of PON in the water column remains slightly too low in spite of the fact that the temporal dynamics of the nitrate and of the ammonium pool are quite well described. We have to conclude that this is due to lateral advective import of either nitrate or PON. Furthermore, in the second half of the two-month simulation period the simulation yields too high ammonium concentrations in the euphotic zone and too low concentrations in the water column below. This may be partly due to the neglect of vertical migration of the zooplankton which was observed after the middle of May.

The results of the simulation suggest that strong herbivorous grazing was responsible for the decay of the bloom. The comparison with the grazing by herbivorous mesozooplankton as estimated from the observations favors the hypothesis that herbivorous microzooplankton was responsible for the breakdown, as was also suggested by Carlotti and Radach (1996).

The depth dependence of the vertical particulate flux obtained from the simulation exhibits the hyperbolic character mostly found in different oceanic regions. The vertical particulate nitrogen flux shows a stronger decrease than generally observed for the particulate carbon flux. This is in correspondence with the observation that there was a remarkable increase of the C/N ratio of POM with depth during FLEX '76.

Further progress in the understanding of the pelagic ecosystem is only possible when

field measurements and modeling work close together. For future measuring campaigns we want to strongly recommend concentration on time series measurements which include the most important constituents of the ecosystem; i.e., also microzooplankton, ammonium and labile dissolved organic compounds. Future model investigations should concentrate on the improvement of the description of the heterotrophic processes (grazing of zooplankton, bacterial metabolism) and of the dynamics of sinking processes of particulate matter.

Acknowledgments. For stimulating discussions and useful hints, we would like to express our gratitude to Dr. H. Baumert, Dr. F. Carlotti, A. Eigenheer, Dr. H. Frey, Dr. H. Friedrich, Dr. M. Krause, H. Lenhart, Dr. A. Moll and M. Regener. This work was kindly supported by the Bundesministerium für Forschung und Technologie (contracts no. 03F0014A and 03F01060A).

REFERENCES

Berger, W. H., K. Fischer, C. Lai and G. Wu. 1988. Ocean carbon flux: global maps of primary production and export production, *in* Biogeochemical cycling and fluxes between the deep euphotic zone and other oceanic realms, NOAA National Undersea Research Program, C. R. Agegian, ed., Res. Rep. 88-1, 131–176.

Billen, G., C. Joiris, L. Meyer-Reil and H. Lindeboom. 1990. Role of bacteria in the North Sea ecosystem. Neth. J. Sea Res., *26,* 265–293.

Brockmann, U. H., K. Eberlein, K. Huber, H.-J. Neubert, G. Radach and K. Schulze. 1984. JONSDAP '76ö: FLEX/INOUT Atlas, Vol. I, II. ICES Oceanographic Data Lists and Inventories, Nos. 63 and 64, Copenhagen, Denmark.

Brockmann, U. H., V. Ittekot, G. Kattner, K. Eberlein and K. D. Hammer. 1983. Release of dissolved organic substances in the course of phytoplankton blooms, *in* North Sea Dynamics, J. Sündermann and W. Lenz, eds., Berlin, Heidelberg, New York: Springer-Verlag, 530–548.

Butler, E. L., E. D. S. Corner and S. M. Marshall. 1970. On the nutrition and metabolism of zooplankton. VIII. Seasonal survey of the nitrogen and phosphorus excretion of Calanus in the Clyde Sea area. J. Mar. Biol. Assoc. U. K., *50,* 525–560.

Carlotti, F. and G. Radach. 1996. Seasonal dynamics of phytoplankton and *Calanus finmarchicus* in the North Sea as revealed by a coupled 1-D model. Limnol. Oceanogr., *43,* 522–539.

Cole, J. C., S. Findlay and M. L. Pace. 1988. Bacterial production in fresh and salt water ecosystems: a cross-system overview. Mar. Ecol. Prog. Ser., *43,* 1–10.

Davies, J. M. and R. Payne. 1984. Supply of organic matter in the northern North Sea during a spring phytoplankton bloom. Mar. Biol., *78,* 315–324.

Ducklow, H. W., D. L. Kirchman, H. L. Quinby, C. A. Carlson and H. G. Dam. 1993. Stocks and dynamics of bacterioplankton carbon during the spring bloom in the eastern North Atlantic Ocean. Deep-Sea Res., *40,* 245–264.

Eberlein, K., G. Kattner, U. Brockmann and K. D. Hammer. 1980. Nitrogen and phosphorus in different water layers at the Central Station during FLEX '76. "Meteor" Reihe A, *22,* 87–98.

Eigenheer, A., W. Kühn and G. Radach. 1996. On the variability of ecosystem box model results caused by mixed layer depth determination. Deep-Sea Res., *43,* 1011–1027.

Fasham, M. J. R. 1993. Modeling the marine biota, *in* The Global Carbon Cycle, M. Heimann, ed., Berlin: Springer, 457–504.

Fasham, M. J. R., H. W. Ducklow and S. M. McKelvie. 1990. A nitrogen-based model of plankton dynamics in the oceanic mixed layer. J. Mar. Res., *48,* 591–639.

Fasham, M. J. R., J. L. Sarmiento, R. D. Slater, H. W. Ducklow and R. Williams. 1993. Ecosystem behaviour at Bermuda station "S" and ocean weather station "India": A general circulation model and observational analysis. Global Biogeochem. Cycles, *7,* 379–415.

Friedrich, H. 1983. Simulation of the thermal stratification at the FLEX central station with a one-dimensional integral model, *in* North Sea Dynamics, J. Sündermann and W. Lenz, eds., Berlin: Springer, 396–411.

Hammer, K. D., K. Eberlein, G. Kattner and U. H. Brockmann. 1983. Fluctuations of dissolved amino acids: a comparison of natural and enclosed phytoplankton populations in the North Sea, *in* North Sea Dynamics, J. Sündermann and W. Lenz, eds., Berlin, Heidelberg, New York: Springer, 559–572.

Hentzschel, G. 1980. Wechselwirkungen bakteriolytischer und saprophytischer Bakterien aus der Nordsee. Mitt. Inst. Allg. Bot. Hamburg, *17,* 113–124.

Hoejerslev, N. K. 1982. Bio-optical properties of the Fladenground: "Meteor"—FLEX '75 and FLEX '76. J. Cons. Int. Explor. Mer., *40,* 272–290.

Hutson, V. 1984. Predator mediated coexistence with a switching predator. Math. Biosc., *68,* 233–246.

Krause, M. and G. Radach. 1980. On the succession of developmental stages of herbivorous zooplankton in the northern North Sea during FLEX '76. I. First statements about the main groups of the zooplankton community. "meteor" Forsch.-Ergebn. *A 22,* 133–149.

—— 1989. On the relations of vertical distribution, diurnal migration and nutritional state of herbivorous zooplankton in the northern North Sea during FLEX '89. Int. Rev. Ges. Hydrobiol., *74,* 371–417.

Kühn, W. 1994. Ein eindimensionales physikalisch-biologisches Modell des pelagischen Stickstoffkreislaufs. Anwendungsfall: Frühjahrsblüte in der nördlichen Nordsee (FLEX '76). Berichte aus dem Zentrum für Meeres—und Klimaforschung, Reihe B, Heft 14, 66 pp.

Lenz, W., J. Ramster and H. Weidemann. 1980. First steps in the realization of the Joint North Sea Data Acquisition Project for 1976 (JONSDAP '76). "Meteor" Reihe B, 3–10.

Martin, J. H., S. E. Fitzwater, R. M. Gordon, C. N. Hunter and S. J. Tanner. 1993. Iron, primary production and carbon-nitrogen flux studies during the JGOFS North Atlantic Bloom Experiment. Deep-Sea Res., II, *40,* 115–134.

Martin, J. H., G. A. Knauer, D. M. Karl and W. W. Broenkow. 1987. VERTEX: carbon cycling in the northeast Pacific. Deep-Sea Res., *34,* 267–285.

Mellor, G. L. 1989. Retrospect on oceanic boundary layer modeling and second moment closure, *in* Parameterization of Small-Scale Processes. P. Müller and D. Henderson, eds., Proc. of the Hawaiian Winter Workshop, Jan. 18–20, 1989, 251–272.

Mellor, G. L. and P. A. Durbin. 1975. The structure and dynamics of the ocean surface mixed layer. J. Phys. Oceanogr., *5,* 718–728.

Mellor, G. L. and T. Yamada. 1974. A hierarchy of turbulence closure models for planetary boundary layers. J. Appl. Meteor., *13,* 1791–1806.

—— 1982. Development of a turbulence closure model for geophysical fluid problems. Rev. Geophys. Space Phys., *20,* 851–875.

Mommaerts, J. P. 1981. Atlas of particulate primary production results from the central station during the FLEX '76 campaign as calculated with a model of photosynthesis-light relationship. Management Unit of the North Sea Model, Ministry of Public Health, I.H.E., Brussels, Belgium.

Morel, A. and R. C. Smith. 1974. Relation between total quanta and total energy for aquatic photosynthesis. Limnol. Oceanogr., *19,* 591–600.

Oguz, T., H. Ducklow, P. Malanotte-Rizzoli, S. Tugral, N.P. Nezlin and U. Unluata. 1996. Simulation of annual plankton productivity cycle in the Black Sea by a one-dimensional physical-biological model. J. Geophys. Res., 107, 16,585–16,599.

O'Neill, R. V., D. L. Deangelis, J. J. Pastor, B. J. Jackson and W. M. Post. 1989. Multiple nutrient limitations in ecological models. Ecol. Model., *46,* 147–163.

Pace, M. L., G. A. Knauer, D. M. Karl and J. H. Martin. 1987. Primary production, new production and vertical flux in the eastern Pacific Ocean. Nature, *325,* 803–804.

Paulson, C. A. and J. J. Simpson. 1977. Irradiance measurements in the upper ocean. J. Phys. Oceanogr., *7,* 952–955.

Radach, G., J. Berg, B. Heinemann and M. Krause. 1984. On the relation of primary production to grazing during the Fladen Ground Experiment 1976 (FLEX '76), *in* Flows of Energy and Materials in Marine Ecosystems, M. J. R. Fasham, ed., NATO Conf. Ser. IV: Marine Sciences, *13,* New York.

Radach, G. and A. Moll. 1993. Estimation of the variability of production by simulating annual cycles of phytoplankton in the central North Sea. Prog. Oceanogr., *31,* 339–419.

Radach, G., J. Trahms and A. Weber. 1980. The chlorophyll development at the central station during FLEX '76. Two data sets. ICES C. M., *C3,* 3–21.

Raschke, A. C., J. Schmetz, M. Kerschgens, G. U. Spohr, U. Pilz and U. Reuter. 1978. Measurements of the radiation budget components over the North Sea. "Meteor" Reihe B, 14–23.

Regener, M. 1992. Deckschichtmodellierung an ausgewählten Standorten in der Nordsee mit dem van-Aken-Modell. Diplomarbeit, Fachbereich Geowissenschaften der Universität Hamburg, 134 S.

Sarmiento, J. L., R. D. Slater, M. J. R. Fasham, H. W. Ducklow, J. R. Toggweiler and G. T. Evans. 1993. A seasonal three-dimensional ecosystem model of nitrogen cycling in the North Atlantic euphotic zone. Global Biogeochem. Cycles, *7,* 417–450.

Schöne, H. K. 1977. Die Vermehrungsrate mariner Planktondiatomeen als Parameter in der Ökosystemanalyse. Habilitationsschrift. Aachen.

Sharples, J. and P. Tett 1994. Modeling the effect of physical variability on the midwater chlorophyll maximum. J. Mar. Res., *52,* 219–238.

Tilman, D. 1982. Resource, Competition and Community Structure, Princeton University Press, Princeton, NJ.

Tupas, L. and I. Koike. 1991. Simultaneous uptake and regeneration of ammonium by mixed assemblages of heterotrophic marine bacteria. Mar. Ecol. Prog. Ser., *70,* 273–282.

Wandschneider, K. 1983. Some biotic factors influencing the succession of diatom species during FLEX '76, *in* North Sea Dynamics J. Sündermann and W. Lenz, eds., Berlin, Heidelberg, New York: Springer-Verlag, 573–583.

Weichart, G. 1980. Chemical changes and primary production in the Fladen Ground area (North Sea) during the first phase of a spring phytoplankton bloom. "Meteor" Forsch.-Ergebn., *A22,* 79–86.

Weigel, P. and E. Hagmeier. 1978. Primary production measurements and the timing of the phytoplankton spring bloom at 58° 55′ N, 0° 32′ E (North Sea) during Fladen Ground Experiment 1976 (FLEX 76). Biologische Anstalt Helgoland, Meeresstation Helgoland. Technical Report.

Wroblewski, J. S. 1977. A model of phytoplankton plume formation during variable Oregon upwelling. J. Mar. Res., *35,* 357–394.

Received: *25 July 1996;* revised: *8 January, 1997.*